Analysis and Improvement of an Anion-Templated Rotaxane Synthesis

by **Christoph A. Schalley***, **Gabriele Silva**, **Carl Friedrich Nising**, and **Petra Linnartz**

Kekulé-Institut für Organische Chemie und Biochemie der Universität Bonn, Gerhard-Domagk-Str. 1, D-53121 Bonn (e-mail: c.schalley@uni-bonn.de)

A series of new rotaxanes with axles different in length was prepared. Following the synthetic protocol utilizing a known anion template effect (*Scheme 1*), surprisingly low yields in the order of 2–5% were obtained (*Scheme 3*), which furthermore significantly depended on the nature of the stopper (*Fig. 1*). Variations in the synthetic procedures and computational results from Monte Carlo simulations allowed us to analyze the origin of these findings: The rotaxane wheel **3** acts as a noncovalently bound 'protecting group' for the stopper nucleophile. The protection of the nucleophilic phenolate O-atom depends much on the steric demands of the stoppers (see **2** *vs.* **10**) which induce different conformations of the wheel. Based on this model, an improved synthetic scheme is suggested.

1. Introduction. – The synthesis of rotaxanes, catenanes, and other types of mechanically interlocked molecules [1] strongly relies on the operation of efficient template effects [2]. There exist different apparoches including *inter alia* those based on the tetrahedral [3] or octahedral [4] coordination geometry of metal ions, π-donor/π-acceptor interactions [5], and H-bonding involving ammoniums ions [6] or neutral amides [7]. The latter is believed to play a crucial role in the formation of a trefoil knot with twelve amide bonds [8]. Recently, *Vögtle* and co-workers reported [9] the high-yield rotaxane synthesis shown in *Scheme 1*, which is based on the recognition of phenolate stopper $\mathbf{2}^-$ within the macrocyclic rotaxane wheel **3**. Two H-bonds bind the trityl phenolate with a surprisingly high binding constant of $K > 10^5$ M^{-1} [9][10] so that the equilibrium is shifted far to the side of the stopper-wheel complex $\mathbf{2}^- \cdot \mathbf{3}$. If the axle-center piece **1** is added to the reaction mixture, the semi-axle **4** is formed – either in a direct reaction of **1** with free $\mathbf{2}^-$, or in a reaction of **1** and $\mathbf{2}^- \cdot \mathbf{3}$ followed by deslipping that occurs due to the much lower strength of the H-bonds formed between the wheel and the semi-axle ether O-atom. Finally, the semi-axle **4** reacts with $\mathbf{2}^- \cdot \mathbf{3}$ to yield the rotaxane $\mathbf{5} \cdot \mathbf{3}$ in up to 95% yield.

For deslipping experiments [11], we attempted to synthesize rotaxanes with axle-center pieces of different lengths, *i.e.*, **9a–j** (obtained from **6** and **7a–j** *via* **8a–j**, see *Scheme 2*), and stoppers of intermediate size such as **10** (*Scheme 3*). Surprisingly, the rotaxane yields decreased dramatically for the rotaxanes discussed here, even to below 5%. Instead, large amounts of the free axle were isolated as the by-product. Three questions arise from these findings: *i*) Why does the yield of rotaxane depend so much on the nature of the stopper? *ii*) If this is due to an unfavorable competition between axle and rotaxane formation, why is the free axle formed so much faster than the rotaxane if **10** is applied as the stopper instead of **2**? *iii*) What is the influence of the center piece?

Scheme 1. *Rotaxane Synthesis as Described in* [9]. Semi-axle **4** is formed under basic conditions from the axle-center piece **1** and tritylphenol stopper **2**. In a second step, **4** reacts with the stopper-wheel complex $\mathbf{2}^{-} \cdot \mathbf{3}$ to yield the rotaxane $\mathbf{5} \cdot \mathbf{3}$.

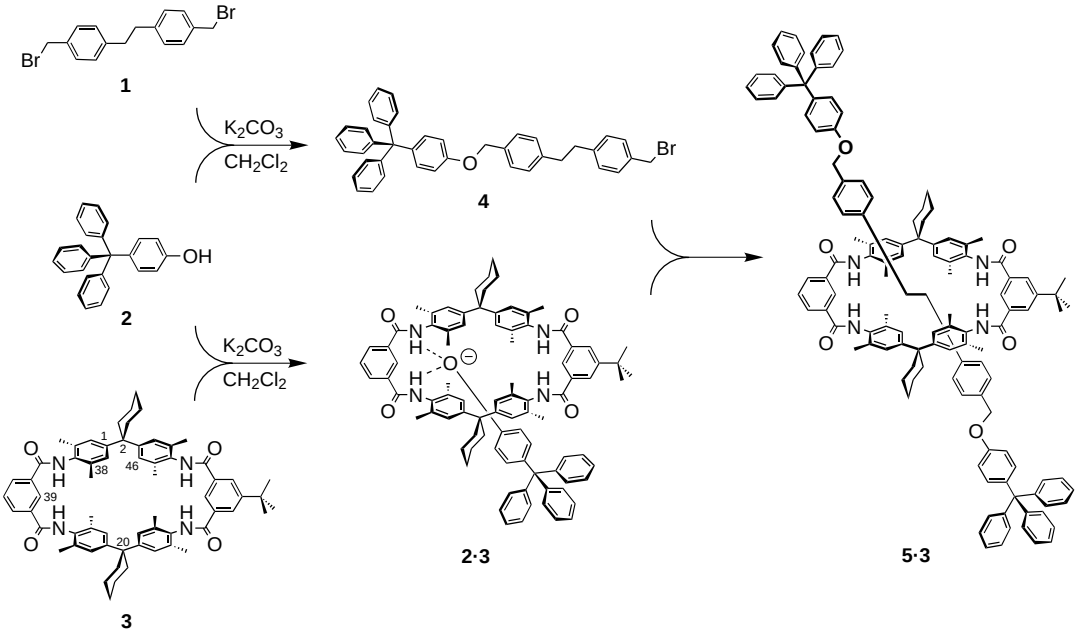

Scheme 2. *Synthesis of the Axle-Center Pieces* **9a**–**j** *with Central Alkyl Chains of Different Lengths*

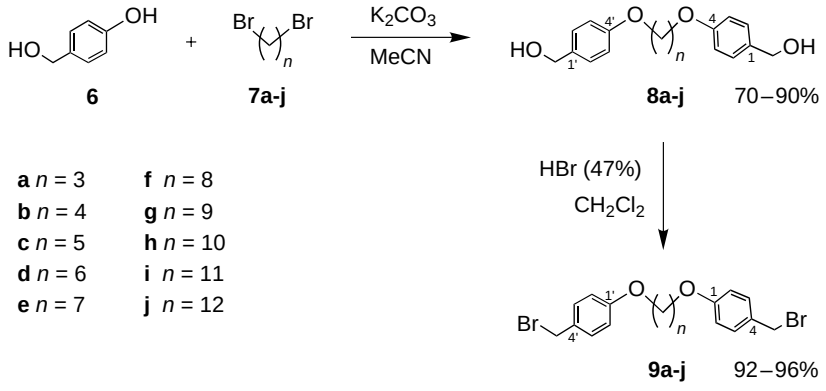

a $n = 3$ **f** $n = 8$
b $n = 4$ **g** $n = 9$
c $n = 5$ **h** $n = 10$
d $n = 6$ **i** $n = 11$
e $n = 7$ **j** $n = 12$

In this contribution, we first describe our attempts to optimize the rotaxane synthesis, including changes of the reaction time, the use of different bases for deprotonation of the phenolate, and the use of silver salts as bromide scavengers. The latter modification strengthens the electrophilicity of the semi-axle by forming the highly reactive benzyl cation almost instantaneously. Subsequently, the stopper-wheel complexes are examined by molecular modeling. Significant geometric differences are

Scheme 3. *Competition between Formation of the Free Axle at a Reaction Rate* k_1 *and the Rotaxane with a Rate* k_2. Note that the equilibrium between the free stopper phenolate **10**$^-$ and the phenolate-wheel complex **10**$^- \cdot$ **3** is completely shifted to the side of the complex as indicated by a binding constant of $K > 10^5$ M^{-1}. Together with the product ratio, one concludes that k_1 must be at least six orders of magnitude higher than k_2. The broken arrow indicates the possibility that the stopper-wheel complex **10**$^- \cdot$ **3** might also react in a way to produce the free axle instead of the rotaxane.

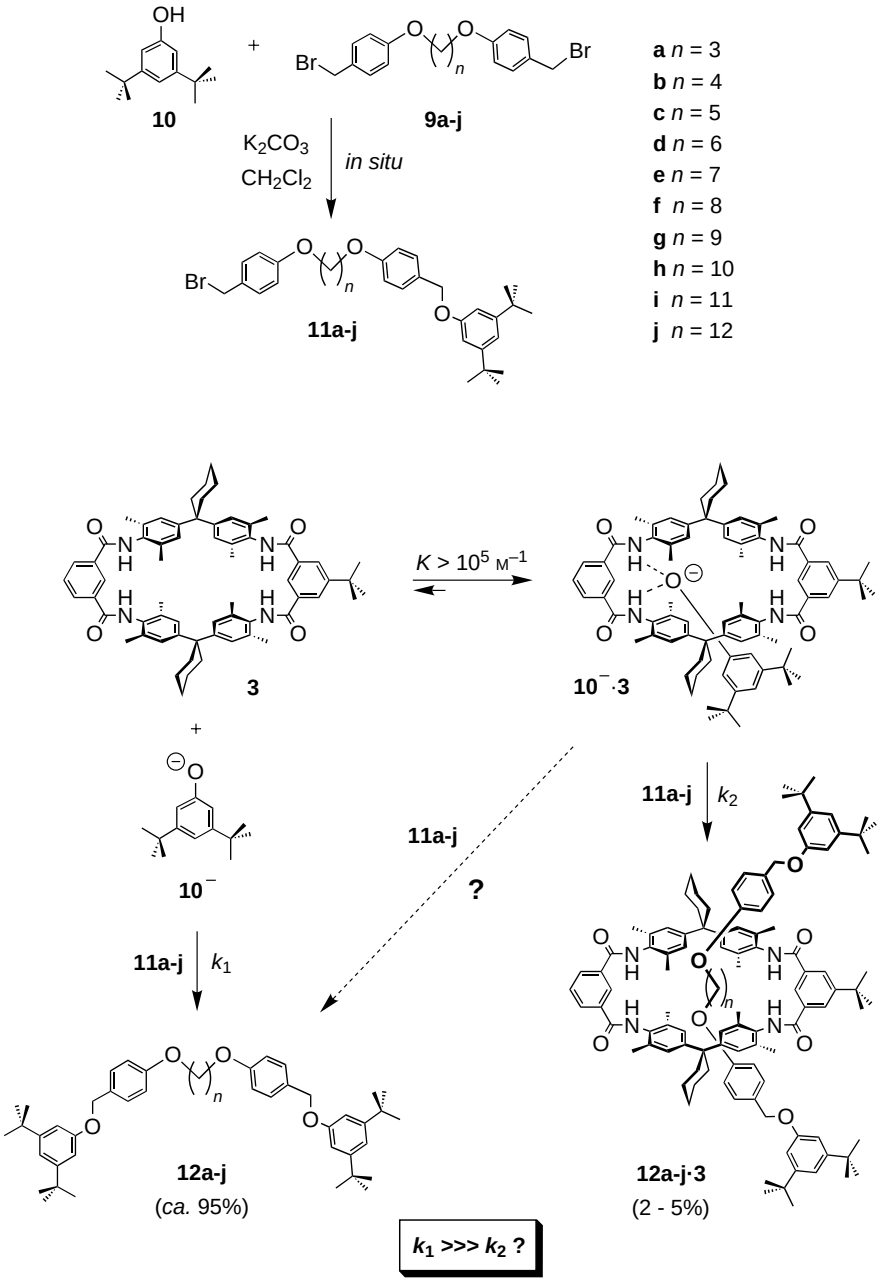

observed for $\mathbf{2}^{-}\cdot\mathbf{3}$ and $\mathbf{10}^{-}\cdot\mathbf{3}$, which are in excellent qualitative agreement with the experimental observations and give answers to the two questions above. The wheel protects the stopper phenolates against attack by the semi-axle electrophile. This effect depends much on the geometric demand of the stopper. Finally, a modified protocol that improves the yield of rotaxanes significantly without much reducing the practicability of the synthetic approach is described.

2. Synthetic Aspects and Attempts Aimed at Improving Rotaxane Yield. – To ensure comparability, the rotaxanes depicted in *Fig. 1* were all repeatedly prepared according to the protocol described by *Vögtle* and co-workers [9] and obtained with the given yields. It is obvious that both the stoppers and the axle-center pieces strongly influence on the rotaxane yields. While $\mathbf{5}\cdot\mathbf{3}$ is formed almost quantitatively, the yield drops significantly to 50–60%, if the smaller di(*tert*-butyl)phenol stopper is used. Analogously, the combination of the tritylphenol stopper with center pieces **9f**–**h** gave much higher yields (30–35%) than the same reaction aiming at rotaxanes $\mathbf{12a}-\mathbf{j}\cdot\mathbf{3}$ by using the smaller stopper **10** (2–5%). Not only the stopper has a significant effect on the yield, also the center piece plays a role, which becomes obvious when comparing rotaxane $\mathbf{5}\cdot\mathbf{3}$ with $\mathbf{14f}-\mathbf{h}\cdot\mathbf{3}$ and $\mathbf{13}\cdot\mathbf{3}$ with $\mathbf{12a}-\mathbf{j}\cdot\mathbf{3}$ (*Fig. 1*).

When we first obtained yields of *ca.* 3% with rotaxane $\mathbf{12a}\cdot\mathbf{3}$, we hypothesized that deslipping of the rotaxane would occur at a high rate and thus would explain the large amount of free axle **12a** formed during the reaction time of six days. However, such a fast deslipping is not in agreement with the corresponding rates of similar rotaxanes [11], which have a half-life at 60° on the order of 50 to 80 h and thus, at room temperature, should be much longer-lived. Nevertheless, the reaction time was varied from two to eight days in an effort to confirm higher yields at shorter time intervals. However, this was not found. Together, these two results rule out deslipping as the reason for the low rotaxane yields with the di(*tert*-butyl)phenol stopper **2**.

Next, the role of the base was examined. It is not quite clear how fast deprotonation of the phenolate occurs when potassium carbonate is used as the base. Definitely, in the solid-liquid two-phase system with CH_2Cl_2, [18]crown-6 or its dibenzo derivative are required as a phase-transfer catalyst. To completely deprotonate the phenol prior to the reaction, stopper **10** was dissolved in CH_2Cl_2, and 1 equiv. of BuLi was added, followed by the wheel **3** (*Scheme 4*,*a*). While the lithium phenolate did not precipitate, the stopper-wheel complex immediately formed a white solid upon addition of the wheel. The precipitate could easily be dissolved again by addition of [15]crown-5 which formed a complex with the Li^{+} ion and thus provided solubility. After addition of the axle-center piece **9a**, the reaction was complete within less than 24 h. The yields of rotaxane $\mathbf{12a}\cdot\mathbf{3}$ and free axle **12a** did not change significantly. Consequently, the base is not the important factor, which can be understood if one assumes a rapid protonation-deprotonation equilibrium prior to a slower, rate-determining nucleophilic displacement reaction.

Finally, the role of the electrophile was tested. Since the reaction of a benzyl bromide with a nucleophile is probably an S_N1-type reaction, the electrophile might play a more important role than the nucleophile. In nonpolar solvents like CH_2Cl_2, however, formation of the benzyl cation is energetically unfavorable, so that addition of a silver salt to precipitate the bromide and replace it with a more weakly binding

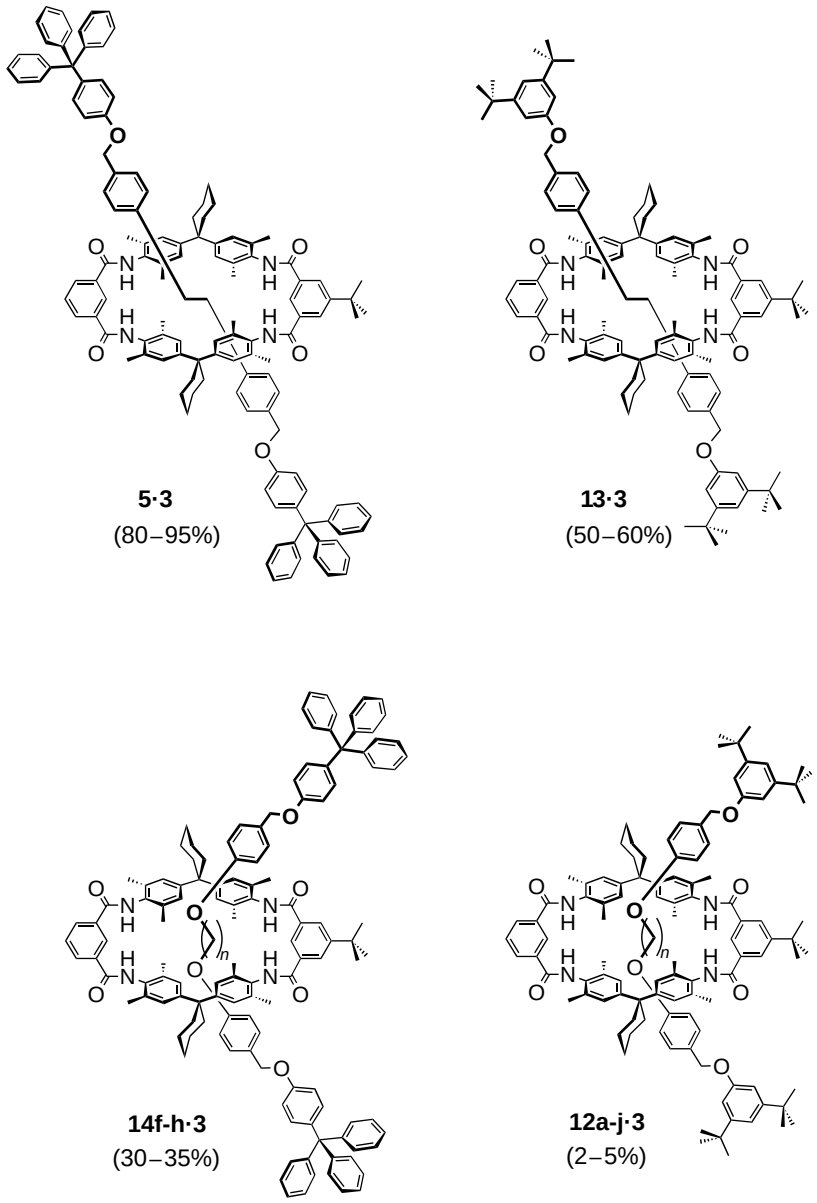

Fig. 1. *Rotaxane yields depending on the stoppers and center pieces.* The yields of **5**·**3** and **13**·**3** are taken from [9] and [11], resp.

counterion can be expected to yield better results. A solution of the stopper-wheel complex $\mathbf{10}^{-}\cdot\mathbf{3}$ was prepared as described above and then treated with the axle-center piece **9a** and 2 equiv. of $AgNO_3$ or $AgBF_4$ as bromide scavengers (*Scheme 4*,*b*). The silver salts did not dissolve in CH_2Cl_2, but upon sonication for 15 min, AgBr was

Scheme 4. *Variations of the Synthetic Protocol Aiming at an Improvement of the Rotaxane Yield*. a) Complete deprotonation of the stopper **10** gives rise to an almost quantitative complex formation with the wheel. b) Addition of a silver salt as bromide scavenger significantly increases the electrophilicity of the center piece by benzyl-cation formation.

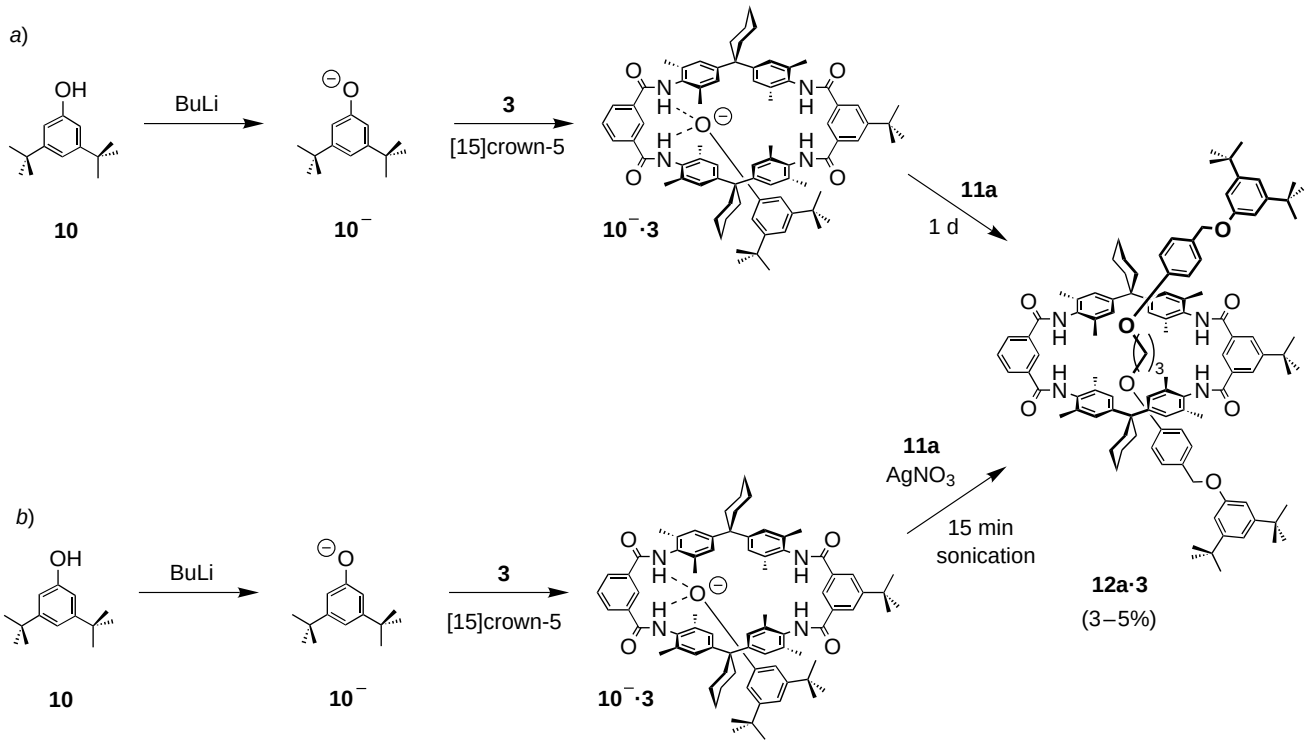

formed concomitantly with the corresponding benzyl cations, which rapidly reacted with the stopper-wheel complex. According to TLC, the reaction was finished within 15 min and again produced the same ratio of rotaxane and free axle. Thus, also the electrophile does not exert significant influence on the products ratio.

From these results, the mechanistic scenario depicted in *Scheme 3* can be derived. *In situ*, the semi-axles **11a–j** are formed from phenol **10** and the center pieces **9a–j**. Simultaneously, the phenolate $\mathbf{10}^-$ forms the stopper-wheel complex $\mathbf{10}^- \cdot \mathbf{3}$ in an equilibrium which is shifted completely to the side of the complex ($K > 10^5$ M^{-1}). To explain an approximate 9:1 ratio of free axles **12a–j** and rotaxanes **12a–j**·**3**, two competing reactions must be taken into account. While the formation of the free axles from the semi-axles and the free phenolate proceeds at a rate k_1, the rotaxane is produced at a much lower rate k_2. Taking into account a lower limit for the binding constant of 10^5 M^{-1} and a product ratio of *ca.* 20:1 in favor of the free axle, k_1 must at least be four to five orders of magnitude higher than k_2, a factor that translates into quite a large difference in the activation barrier (ΔE_A). Two possible effects might contribute to such an effect: *i*) The phenolate is H-bound, if complexed to the amide protons of the tetralactam macrocycle. This might reduce the nucleophilicity of the phenolate O-atom. However, this effect should similarly affect both stoppers **2** and **10**. Furthermore, in an S_N1 displacement, nucleophilicity is not expected to be the dominant factor. *ii*) Thus, steric effects might be invoked to rationalize the findings. The phenolate O-atom can be expected to be buried within the cavity of the macrocycle so that the attack path of the electrophile is obstructed by the wheel. Of course, this analysis is based on the *Arrhenius* equation and assumes that the pre-exponential factor of both reactions is closely similar. This assumption is, however, probably not entirely correct, because the pre-exponential factor contains entropic contributions to the activation barrier, which may be different for the free phenolate as compared to the stopper-wheel complex. Nevertheless, the difference in E_A must be significant with the consequence that the competition between the two reactions characterized by k_1 and k_2 is likely not the only reason for the observed product ratio.

3. Molecular Modeling. – To examine the steric requirements of the stopper-wheel complexes $\mathbf{2}^- \cdot \mathbf{3}$ and $\mathbf{10}^- \cdot \mathbf{3}$ in greater detail, force-field calculations were performed with the Amber* force field [12] as implemented in the MacroModel 7.1 program package [13]. For a detailed mechanistic picture, one, of course, would have to calculate not only the minima on the potential-energy surfaces, but also the transition structures. This is, however, not feasible with molecules of the size and flexibility of the complexes under discussion. Nevertheless, searching for the energetically most favorable conformations of the stopper-wheel complexes may serve as a good approximation and may at least give some indication why the reactivities of the two stoppers differ so much.

To find those lowest-energy conformations (*Figs. 2* and *3*), Monte Carlo conformational searches were carried out in which 1000 structures were calculated for each of the complexes. The differences between the two structures are clearly visible. While the phenolate O-atom of the tritylphenol-derived stopper $\mathbf{2}^-$ is well-accessible for the incoming electrophile in $\mathbf{2}^- \cdot \mathbf{3}$ (*Fig. 2*, top left), it is buried under the Me groups of the wheel's dimethylaniline subunits in $\mathbf{10}^- \cdot \mathbf{3}$ (*Fig. 3*, top left). Viewed from the opposite

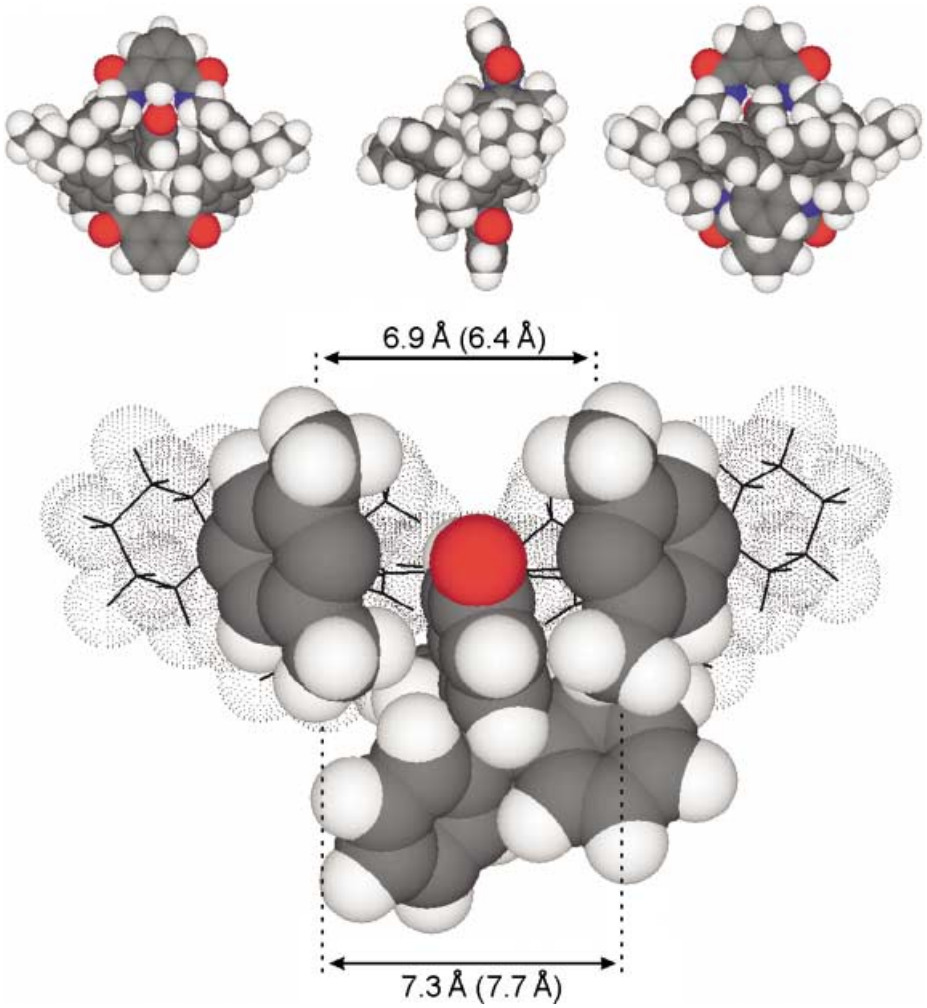

Fig. 2. *Lowest-energy conformation of the tritylphenolate-wheel complex* $\mathbf{2}^- \cdot \mathbf{3}$ *out of a 1000-step Monte Carlo conformational search* (Amber* force field as implemented in the MacroModel 7.1 program package). The ^{t}Bu group attached to the wheel is omitted. The complex is shown in the direction of the attacking electrophile (top left), from the side (top middle), and from the side opposed to the electrophile (top right). The phenolate O-atom – although buried within the cavity is somewhat exposed towards attack of the electrophile. The bottom picture shows the insertion of the stopper into the wheel. The frontal isophthalic acid is omitted to provide an unobstructed view. *Van der Waals* radii of the remote wheel atoms are shown as dotted surfaces. The numbers give distances in Å between the two pairs of Me groups as indicated; numbers in parentheses are average distances of the thirty most favorable conformations).

direction (*Figs. 2* and *3*, top right), *i.e.*, the side blocked by the stopper itself, the phenolate O-atom of $\mathbf{2}^- \cdot \mathbf{3}$ is hardly visible, while that of $\mathbf{10}^- \cdot \mathbf{3}$ is much more freely exposed to the environment. Consequently, attack of the electrophilic semi-axle seems to be preferred through the wheel for $\mathbf{2}^- \cdot \mathbf{3}$, while the formation of the axle might well

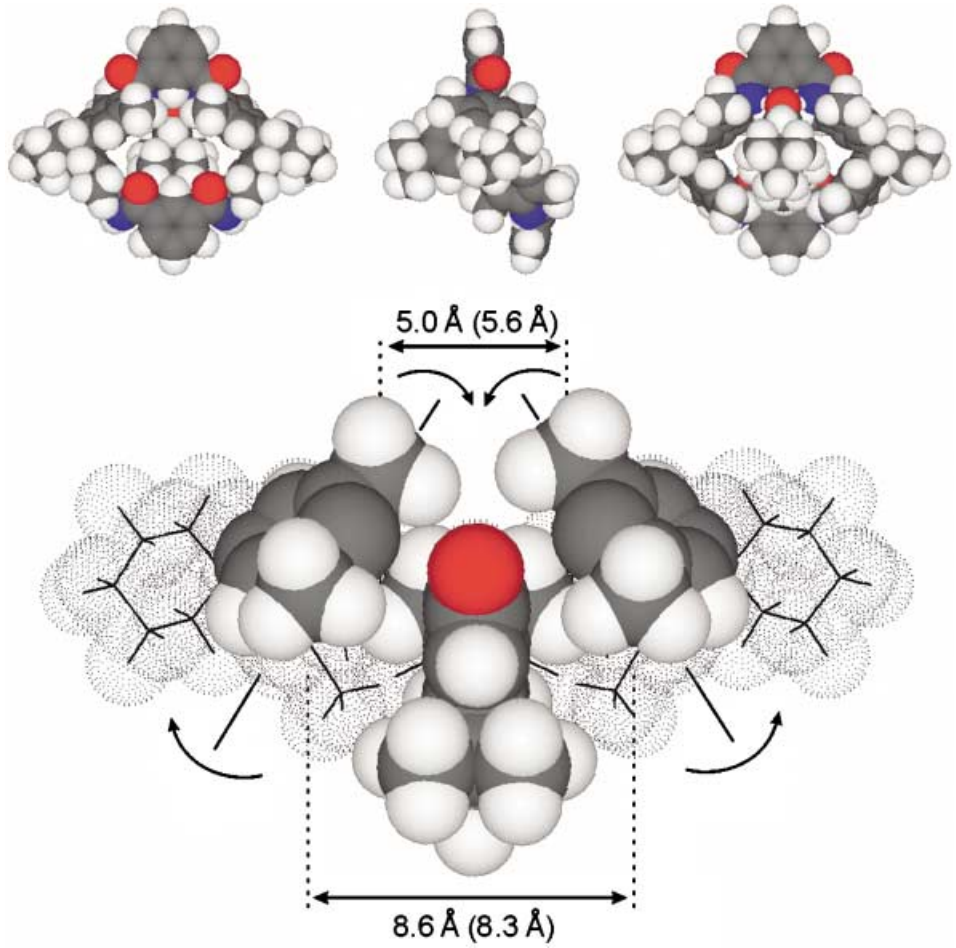

Fig. 3. *Lowest-energy conformation of the di*(tert-*butyl*)*phenolate-wheel complex* **10**$^{-}$ · **3** *shown in analogy to* Fig. 2. The complex offers a much more narrow attack path to the electrophile.

occur on the same side of the wheel for **10**$^{-}$ · **3**. This process would lead to the free axle, while **2**$^{-}$ · **3** would yield the rotaxane.

It is interesting to analyze the two structures in some more detail. The stoppers induce quite different conformations of the wheel. For **2**$^{-}$ · **3**, the two isophthalic acid subunits are not parallel (*Fig. 2*, top middle), with the one involved in H-bonding being tilted by *ca*. 40° against the other one. In **10**$^{-}$ · **3**, both isophthalic acid building blocks are more or less parallel (*Fig. 3*, top middle). Even more telling is the view at the bottom of *Figs 2* and *3*. The two dimethylaniline rings neighboring the H-bonding site are almost parallel for **2**$^{-}$ · **3**, opening a rather comfortable 'access road' for the semi-axle. Instead, these rings are conically tilted with the two upper Me groups hindering the electrophile to react in a rotaxane-producing way. These differences can be quantified by the distances between the Me groups as indicated in *Figs. 2* and *3*. While

the C···C distance is almost 7 Å for complex $\mathbf{2}^{-}\cdot\mathbf{3}$, it is almost 2 Å smaller for $\mathbf{10}^{-}\cdot\mathbf{3}$. *Vice versa*, the two Me groups on the other side of the wheel are more distant in the latter case than for $\mathbf{2}^{-}\cdot\mathbf{3}$ (8.6 Å *vs.* 7.3 Å).

The differences between the two conformations become even clearer when one takes a closer look at the H-bonding pattern (*Fig. 4*). The nucleophilic, negatively charged phenolate O-atom bears three lone pairs, two of which are involved in the formation of the two H-bonds to the two amide protons. The third, which is likely the reactive one, forms the axle with the semi-axle benzyl cation. The two different conformations also differ with respect to the location of this lone pair. For $\mathbf{2}^{-}\cdot\mathbf{3}$, it is positioned exactly as required for productive rotaxane formation (arrow in *Fig. 4*,*a*), while it is located on the same side of the wheel as the stopper for $\mathbf{10}^{-}\cdot\mathbf{3}$ (*Fig. 4*,*b*). Consequently, for the di(*tert*-butyl)phenol stopper, formation of the free axle will be preferred even from the stopper-wheel complex.

These arguments are in excellent agreement with the experimental findings and offer a good rationalization for the differences in the behavior of the two stoppers. However, one might argue that a simple force-field calculation might be somewhat uncertain. Therefore, we looked for other conformation among the higher-energy structures optimized during the Monte Carlo search. Indeed, two families of conformations exist for both stopper-wheel complexes[1]), of which the two structures discussed above are representative. However, these structures are not evenly distributed over the energy range of the calculations. While for $\mathbf{2}^{-}\cdot\mathbf{3}$, structures with a conformation similar to that depicted in *Fig. 2* dominate, in particular for lower energies (the first 26 structures all belong to this family and have calculated energies of formation in a range of 26 kJ/mol above the lowest-energy conformer), for $\mathbf{10}^{-}\cdot\mathbf{3}$, more geometries like that in *Fig. 3* are found at lower energies, while conformations similar to that in *Fig. 2* become more frequent at higher energies. Six of those structures similar to that in *Fig. 3* exist among the lowest ten conformers, but only eight among the first 30 conformers. This is also reflected in the Me···Me distances. The values in parentheses give the average distances for the thirty lowest-energy conformers of each complex. Still, there is a difference between the two complexes of almost 1 Å (6.4 Å for $\mathbf{2}^{-}\cdot\mathbf{3}$ *vs.* 5.6 Å for $\mathbf{10}^{-}\cdot\mathbf{3}$). Thus, one can expect that $\mathbf{2}^{-}\cdot\mathbf{3}$ more frequently populates the open conformation that leads to the rotaxane, while $\mathbf{10}^{-}\cdot\mathbf{3}$ prefers the other geometry that forms the free axle.

Of course, this picture does not rule out the possibility that the free stopper reacts more quickly than the stopper-wheel complex. However, the scenario developed with the help of molecular modeling offers a second alternative, which avoids the assumption of the large difference in activation energies for axle and rotaxane formation. Instead of competition between the free stopper and the stopper-wheel complex, the reaction may also involve competition between the two different conformations of the stopper-wheel complex, one giving rise to the rotaxane, the other

---

[1]) A third family was found among the structures higher in energy for $\mathbf{10}^{-}\cdot\mathbf{3}$ in which the stopper is not inserted into the wheel with one ^{t}Bu group as in *Fig. 3*, but rotated by 90° and positioned in a coplanar fashion relative to the wheel. In these conformations, the two ^{t}Bu groups of the stopper are located in close proximity to the two Me groups of the neighboring dimethylaniline rings and force these two aromatic rings into a conical conformation similar to that shown in *Fig. 3*. Consequently, these conformations will have an effect similar to that of those represented by the structure shown in *Fig. 3*.

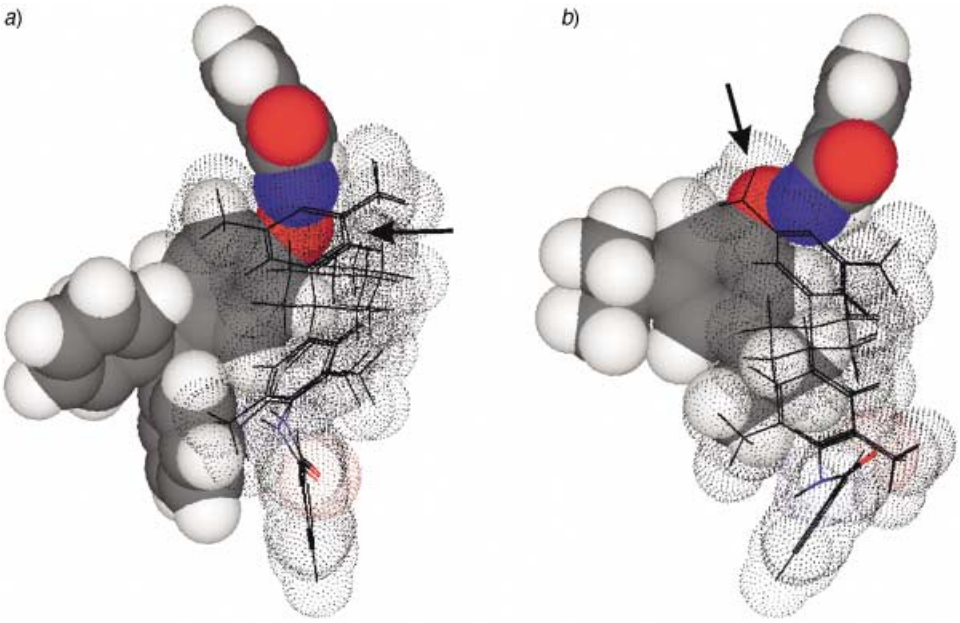

Fig. 4. *Stopper-wheel complexes* a) $\mathbf{2}^{-} \cdot \mathbf{3}$ *and* b) $\mathbf{10}^{-} \cdot \mathbf{3}$ *in a side view with the remote parts of the wheel shown as dotted* Van der Waals *surfaces.* The solid atoms represent the stoppers and the isophthalic diamide subunit involved in H-bonding. The arrows point to the free electron pair of the phenolate O-atom not H-bound to the two amide protons and thus indicate the preferred attack path of the electrophile.

yielding the free axle (dotted arrow in *Scheme 3*). The observed product distributions may nevertheless be due to a combination of both effects.

4. The Axle-Center Pieces. – Although we cannot give as nearly detailed a rationalization for the influence of the axle-center pieces, one can, of course, speculate why the yields are smaller for the longer, ether-bearing center pieces in **12a**–**j** · **3** and **14f**–**h** · **3** (*Fig. 1*). One issue, certainly, is flexibility. The transition structure for the reaction giving rise to the rotaxanes is expected to be entropically unfavorable, because it requires a rather precise arrangement of the reaction partners inside the cavity of the macrocycle. Consequently, a rather flexible center piece might require that a larger number of rotations around the central single bonds be frozen out and, thus, would be entropically disfavored over a less-flexible center piece such as **1**. Another effect might be due to differences in solvation. While the center pieces **9a**–**j** bear ether groups that make the attached aromatic rings somewhat more electron rich, such groups are absent in **1**. However, for the time being, the details of these influences remain unknown and speculative.

5. A Synthetic Protocol Improving Rotaxane Yields and Practicability. – As neither changes in the reaction time nor the use of different bases or silver salts as bromide scavengers led to an improved rotaxane yield, there was not much room left for a further optimization. More competitive solvents reduce the strength of the H-bonds in

the stopper-wheel complex and thus have a negative influence on the template effect. Consequently, CH_2Cl_2 is the best compromise between low polarity and the absence of H-bond donors or acceptors on the one hand and the solubility of the reaction partners on the other. According to our experience, other solvents do not increase the yield of rotaxane, because either the components are not soluble enough or the solvents are too competitive and interfere with the template effect by H-bond formation.

A yield of 2–5% in a synthesis of a rotaxane is nevertheless rather disappointing, in particular as the preparation of the wheel involves a macrocyclization step that proceeds at rather low yields (30–50%) as well and requires a tedious chromatographic purification to separate the wheel from catenanes, larger wheels, and polymers formed simultaneously, even under high-dilution conditions. Thus, we searched for other ways to improve the synthetic scheme. One possibility is, of course, to not only isolate the rotaxane from the reaction mixture, but to also recover the remaining portion of the macrocycle and recycle it in another reaction. However, this procedure still requires quite an effort during chromatography with very high consumption of stationary phase and solvents.

Since the axle-center pieces and the stoppers are either commercially available at low cost or straighforward to produce in larger quantities, the wheel is the most precious material required for the synthesis of the rotaxanes. Thus, it would be a significant improvement, if an excess of center piece and stopper would lead to an increased consumption of the wheel. Relative to the amount of wheel used as the reactant, higher yields would be achieved; simultaneously, also an accordingly large excess of the free axle would be formed, which can, however, be separated from the rotaxane by chromatography due to a difference in the R_f values of *ca.* 0.5 (rotaxane R_f 0.2–0.3 and axle R_f 0.7–0.75 in CH_2Cl_2/AcOEt 30:1).

With some optimization, the rotaxane yields could be increased significantly to 20–25% relative to the wheel by adding six additional portions of 1 equiv. of the center piece and 2 equiv. of the stopper to the reaction mixture at equivalent time intervals of several hours (*Protocol B*, see *Exper. Part*). The stepwise procedure turned out to work somewhat better than the addition of the total amount of all the reactants at the beginning of the reaction. Of course, adding more aliquots of center pieces and stoppers (as long as there is an excess of base present) may even give rise to higher yields. To find the optimum for a given rotaxane, many factors should be taken into account, *e.g.*, the costs of the stoppers and center pieces, chromatographic separability of the rotaxane from the excess of the free axle, deslipping as a competing reaction for stoppers of smaller sizes, or the reaction time.

6. Conclusions. – Starting from a notoriously unsuccessful synthesis of rotaxanes, we found a surprising influence of stopper geometry on the rotaxane yield. An analysis of the template effect by a series of experiments and Monte Carlo calculations offers an interesting and conclusive rationalization for these findings. Based on this model, a synthetic protocol improving the yield and practicability was developed and used for the synthesis of new rotaxanes with different axle lengths.

We are grateful to Prof. *Fritz Vögtle* for generous support and fruitful discussions. *C.A.S.* thanks the *Fonds der Chemischen Industrie* for a *Liebig Fellowship* and the *Deutsche Forschungsgemeinschaft* for financial support. *C.F.N.* is grateful to the *Studienstiftung des Deutschen Volkes* for a fellowship.

Experimental Part

Monte Carlo Conformational Searches. The two stopper-wheel complexes $\mathbf{2}^- \cdot \mathbf{3}$ and $\mathbf{10}^- \cdot \mathbf{3}$ were examined with the Amber* force field [12]. The lowest-energy conformers out of 1000 structures were determined with the Monte Carlo algorithm as implemented in the MacroModel 7.1 program package [13]. Closure bonds were placed in the macrocycle (one of the amide bonds) and the two spirocyclohexane moieties. While the aromatic rings and the amide moieties were constrained to planarity, all single bonds (with the exception of the Me groups) were selected to allow rotations into other conformations. Finally, phenolate and wheel were treated as independent molecules able to move relative to each other. In order not to increase the number of degrees of freedom more than necessary, the *t*Bu group attached to the wheel was omitted. At the same time, this symmetrized the wheel so that no distinction between the two possible binding sides was necessary. The energy range for structures to store in the output file was set to 50 kJ/mol above the lowest-energy conformer.

General. The 4-(triphenylmethyl)phenol (**2**) and 3,5-di(*tert*-butyl)phenol (**10**) were used as purchased from *Lancaster* and *Aldrich*, resp. Macrocycle **3** [14], compounds **8a**–**c, 9a**, and **9b** [15] and rotaxanes $\mathbf{5} \cdot \mathbf{3}$ [9] and $\mathbf{13} \cdot \mathbf{3}$ [11] were synthesized according to well-established literature procedures. CC = column chromatography. NMR Spectra: *Bruker* instruments at 250, 300, or 400 MHz for ^{1}H and 62.5, 75, or 100 MHz for ^{13}C; solvent signal as internal standard; δ in ppm, J in Hz; in general, the formation of a rotaxane led to upfield shifts of the signals for the aromatic protons in the axle-center pieces due to the anisotropy of the aromatic rings incorporated in the wheel (signals easily detected at δ(H) *ca.* 6.0 and 6.7) ppm; chx = spirocyclohexane moieties. EI-, FAB- (*Kratos Concept 1 H*) and MALDI-TOF (*Micromass MALDI-TofSpec-E*) mass spectra: in *m/z* (rel. %); standard matrices 3-nitrobenzyl alcohol and 2,5-dihydroxybenzoic acid, resp.; isotope patterns in MALDI-MS (not superimposed by fragmentations such as H losses) in excellent agreement with calc. patterns based on the elemental composition and natural isotope abundances; signals present for the protonated or sodiated wheel in all MALDI and FAB-MS of rotaxanes, due to partial deslipping upon ionization or formed from the rotaxane loss of one stopper and dethreading of the remaining semi-axle. Elemental analyses were unsatisfying due to unavoidable problems, NMR-detectable inclusion of solvent molecules in the wax-like rotaxanes.

Compounds **8a**–**j**: *General Procedure.* A mixture of 4-hydroxybenzyl alcohol (0.1 mol), the corresponding 1,ω-dibromoalkane **7a**–**j** (0.05 mol) and K_2CO_3 (0.2 mol) in MeCN (500 ml) was refluxed for 24 h. After cooling to r.t., the MeCN was evaporated and the residue partitioned between H_2O and CH_2Cl_2. The aq. phase was extracted several times with CH_2Cl_2 and the combined org. phase dried (MgSO) and evaporated. Compounds **8a**–**j** precipitated as white solids and were purified by recrystallization from acetone.

4,4′-[Hexane-1,6-diylbis(oxy)]bis[benzenemethanol] (**8d**). ^{1}H-NMR (250 MHz, $CDCl_3/CD_3OD$ 2:1): 1.32–1.40 (*m*, 2 CH_2); 1.55–1.70 (*m*, 2 CH_2); 3.85 (*t*, 2 CH_2O); 4.41 (*s*, 2 CH_2OH); 6.73 (*AA′* of *AA′XX′*, $^3J = 8.6$, 4 arom. H); 7.15 (*XX′* of *AA′XX′*, $^3J = 8.6$, 4 arom. H). ^{13}C-NMR (62.5 MHz, $CDCl_3/CD_3OD$ 2:1): 160.1; 134.9; 130.5; 116.1; 69.7; 66.0; 31.0; 27.6. FAB-MS ($C_{20}H_{26}O_4$): 330.2 (15, $M^{+\bullet}$), 313.2 (100, $[M + H - H_2O]^+$).

4,4′-[Heptane-1,7-diylbis(oxy)]bis[benzenemethanol] (**8e**). ^{1}H-NMR (300 MHz, $CDCl_3/CD_3OD$ 2:1): 1.30–1.44 (*m*, 3 CH_2); 1.52–1.71 (*m*, 2 CH_2); 3.87 (*t*, 2 CH_2O); 4.45 (*s*, 2 CH_2OH); 6.75 (*AA′* of *AA′XX′*, $^3J = 8.6$, 4 arom. H); 7.18 (*XX′* of *AA′XX′*, $^3J = 8.6$, 4 arom. H). ^{13}C-NMR (75 MHz, $CDCl_3/CD_3OD$ 2:1): 160.3; 134.9; 130.3; 116.2; 69.8; 66.0; 30.9; 30.8; 27.7. FAB-MS: 344.1 (5, $C_{21}H_{28}O_4^+$; $M^{+\bullet}$), 327.1 (100, $[M + H - H_2O]^+$).

4,4′-[Octane-1,8-diylbis(oxy)]bis[benzenemethanol] (**8f**). ^{1}H-NMR (250 MHz, $CDCl_3/CD_3OD$ 2:1): 1.30–1.48 (*m*, 4 CH_2); 1.58–1.70 (*m*, 2 CH_2); 3.82 (*t*, 2 CH_2O); 4.42 (*s*, 2 CH_2OH); 6.76 (*AA′* of *AA′XX′*, $^3J = 8.6$, 4 arom. H); 7.13 (*XX′* of *AA′XX′*, $^3J = 8.6$, 4 arom. H). ^{13}C-NMR (62.5 MHz, $CDCl_3/CD_3OD$ 2:1): 159.5; 134.7; 129.8; 116.1; 70.5; 66.2; 30.3; 30.2, 27.1. FAB-MS: 358.2 (4, $C_{22}H_{30}O_4^+$; $M^{+\bullet}$), 341.2 (100, $[M + H - H_2O]^+$).

4,4′-[Nonane-1,9-diylbis(oxy)]bis[benzenemethanol] (**8g**). ^{1}H-NMR (250 MHz, $CDCl_3/CD_3OD$ 2:1): 1.32–1.71 (*m*, 7 CH_2); 3.90 (*t*, 2 CH_2O); 4.60 (*s*, 2 CH_2OH); 6.92 (*AA′* of *AA′XX′*, $^3J = 8.6$, 4 arom. H); 7.25 (*XX′* of *AA′XX′*, $^3J = 8.6$, 4 arom. H). ^{13}C-NMR (62.5 MHz, $CDCl_3/CD_3OD$ 2:1): 160.2; 134.7; 130.0; 116.4; 69.7; 66.0; 29.9; 29.8; 29.7; 27.7. FAB-MS: 372.0 (3, $C_{23}H_{32}O_4^+$; $M^{+\bullet}$), 355.0 (100, $[M + H - H_2O]^+$).

4,4′-[Decane-1,10-diylbis(oxy)]bis[benzenemethanol] (**8h**). ^{1}H-NMR (300 MHz, $CDCl_3/CD_3OD$ 2:1): 1.22–1.46 (*m*, 6 CH_2); 1.64–1.80 (*m*, 2 CH_2); 3.91 (*t*, 2 CH_2O); 4.50 (*s*, 2 CH_2OH); 6.86 (*AA′* of *AA′XX′*, $^3J =$ 8.6, 4 arom. H); 7.22 (*XX′* of *AA′XX′*, $^3J = 8.6$, 4 arom. H). ^{13}C-NMR (75 MHz, $CDCl_3/CD_3OD$ 2:1): 158.9; 133.6; 128.9; 114.8; 68.5; 64.5; 29.9; 29.8; 29.7; 26.4. FAB-MS: 386.3 (5, $C_{24}H_{34}O_4^+$; $M^{+\bullet}$), 369.2 (100, $[M + H - H_2O]^+$).

4,4′-[Undecane-1,11-diylbis(oxy)]bis[benzenemethanol] (**8i**). ^{1}H-NMR (300 MHz, $CDCl_3/CD_3OD$ 2:1): 1.25–1.47 (*m*, 7 CH_2); 1.60–1.77 (*m*, 2 CH_2); 3.87 (*t*, 2 CH_2O); 4.46 (*s*, 2 CH_2OH); 6.77 (*AA′* of *AA′XX′*, ^3J = 8.6, 4 arom. H); 7.15 (*XX′* of *AA′XX′*, ^3J = 8.6, 4 arom. H). ^{13}C-NMR (75 MHz, $CDCl_3/CD_3OD$ 2:1): 160.3; 134.9; 130.3; 116.2; 69.9; 66.0; 31.2; 31.2; 31.1; 31.0; 30.4; 29.8; 27.7. FAB-MS: 400.2 (3, $C_{25}H_{36}O_4^+$; $M^{+\bullet}$), 383.2 (100, $[M+H-H_2O]^+$).

4,4′-[Dodecane-1,12-diylbis(oxy)]bis[benzenemethanol] (**8j**). ^{1}H-NMR (300 MHz, $CDCl_3/CD_3OD$ 2:1): 1.22–1.46 (*m*, 8 CH_2); 1.62–1.80 (*m*, 2 CH_2); 3.91 (*t*, 2 CH_2O); 4.47 (*s*, 2 CH_2OH); 6.82 (*AA′* of *AA′XX′*, ^3J = 8.6, 4 arom. H); 7.21 (*XX′* of *AA′XX′*, ^3J = 8.6, 4 arom. H). ^{13}C-NMR (75 MHz, $CDCl_3/CD_3OD$ 2:1): 158.9; 133.5; 128.9; 114.8; 68.5; 64.5; 29.9; 29.9; 29.8; 29.6; 29.4; 26.4. FAB-MS: 414.2 (4, $C_{26}H_{38}O_4^+$; $M^{+\bullet}$), 397.2 (100, $[M+H-H_2O]^+$).

Compounds **9a**–**j**. *General Procedure* [15]. Compounds **8a**–**j** (20 mmol) were added to a two-phase system of 47% HBr soln. (50 ml) and CH_2Cl_2 (150 ml) and stirred rapidly for 1 h. After extraction of the mixture with CH_2Cl_2, the org. layers were washed with sat. $NaHCO_3$ soln. and brine and dried ($MgSO_4$). After evaporation, the remaining solids were immediately used for rotaxane synthesis.

1,1′-[Pentane-1,5-diylbis(oxy)]bis[4-(bromomethyl)benzene] (**9c**). ^{1}H-NMR (300 MHz, $CDCl_3$): 1.50–1.60 (*m*, 1 CH_2); 1.75–1.90 (*m*, 2 CH_2); 3.95 (*t*, 2 CH_2O); 4.45 (*s*, 2 CH_2Br); 6.89 (*AA′* of *AA′XX′*, ^3J = 8.7, 4 arom. H); 7.30 (*XX′* of *AA′XX′*, ^3J = 8.7, 4 arom. H). ^{13}C-NMR (75 MHz, $CDCl_3$): 159.6; 130.8; 130.2; 115.2; 68.2; 34.4; 29.4; 23.1. EI-MS (70 eV): 444 (2), 442 (5), 440 (2, $C_{19}H_{22}Br_2O_2^+$; $M^{+\bullet}$), 363 (69), 361 (70, $[M-Br]^+$), 282 (2, $[M-2Br]^{+\bullet}$), 257 (29), 255 (27, $[BrCH_2C_6H_4OC_5H_{10}]^+$), 107 (100, $[HOC_6H_4CH_2]^+$).

1,1′-[Hexane-1,6-diylbis(oxy)]bis[4-(bromomethyl)benzene] (**9d**). ^{1}H-NMR (250 MHz, $CDCl_3$): 1.51–1.63 (*m*, 2 CH_2); 1.72–1.88 (*m*, 2 CH_2); 3.90 (*t*, 2 CH_2O); 4.38 (*s*, 2 CH_2Br); 6.75 (*AA′* of *AA′XX′*, ^3J = 8.7, 4 arom. H); 7.33 (*XX′* of *AA′XX′*, ^3J = 8.7, 4 arom. H). ^{13}C-NMR (62.5 MHz, $CDCl_3$): 160.2; 130.9; 130.1; 115.5; 68.8; 33.9; 29.5; 23.1. EI-MS (70 eV): 458 (3), 456 (6), 454 (3, $C_{20}H_{24}Br_2O_2^+$; $M^{+\bullet}$), 377 (39), 375 (40, $[M-Br]^+$), 296 (5, $[M-2Br]^{+\bullet}$), 107 (100, $[HOC_6H_4CH_2]^+$).

1,1′-[Heptane-1,7-diylbis(oxy)]bis[4-(bromomethyl)benzene] (**9e**). ^{1}H-NMR (300 MHz, $CDCl_3$): 1.51–1.63 (*m*, 3 CH_2); 1.70–1.89 (*m*, 2 CH_2); 3.85 (*t*, 2 CH_2O); 4.43 (*s*, 2 CH_2Br); 6.90 (*AA′* of *AA′XX′*, ^3J = 8.7, 4 arom. H); 7.31 (*XX′* of *AA′XX′*, ^3J = 8.7, 4 arom. H). ^{13}C-NMR (75 MHz, $CDCl_3$): 159.6; 130.8; 130.1; 115.1; 68.4; 34.4; 29.6; 29.5; 26.3. EI-MS: (70 eV): 472 (1), 470 (2), 468 (1, $C_{21}H_{26}Br_2O_2^+$; $M^{+\bullet}$), 391 (59), 389 (61, $[M-Br]^+$), 310 (4, $[M-2Br]^{+\bullet}$), 107 (100, $[HOC_6H_4CH_2]^+$).

1,1′-[Octane-1,8-diylbis(oxy)]bis[4-(bromomethyl)benzene] (**9f**). ^{1}H-NMR (250 MHz, $CDCl_3$): 1.50–1.57 (*m*, 4 CH_2); 1.69–1.85 (*m*, 2 CH_2); 3.91 (*t*, 2 CH_2O); 4.49 (*s*, 2 CH_2Br); 6.85 (*AA′* of *AA′XX′*, ^3J = 8.7, 4 arom. H); 7.29 (*XX′* of *AA′XX′*, ^3J = 8.7, 4 arom. H). ^{13}C-NMR (62.5 MHz, $CDCl_3$): 159.5; 131.0; 130.2; 115.3; 68.3; 34.4; 29.6; 29.5; 26.3. EI-MS (70 eV): 486 (2), 484 (4), 482 (2, $C_{22}H_{28}Br_2O_2^+$; $M^{+\bullet}$), 405 (65), 403 (64, $[M-Br]^+$), 324 (6, $[M-2Br]^{+\bullet}$), 107 (100, $[HOC_6H_4CH_2]^+$).

1,1′-[Nonane-1,9-diylbis(oxy)]bis[4-(bromomethyl)benzene] (**9g**). ^{1}H-NMR (250 MHz, $CDCl_3$): 1.50–1.90 (*m*, 7 CH_2); 3.95 (*t*, 2 CH_2O); 4.49 (*s*, 2 CH_2Br); 6.85 (*AA′* of *AA′XX′*, ^3J = 8.7, 4 arom. H); 7.25 (*XX′* of *AA′XX′*, ^3J = 8.7, 4 arom. H). ^{13}C-NMR (62.5 MHz, $CDCl_3$): 159.5; 130.5; 129.8; 115.0; 68.5; 34.6; 29.6; 29.5; 29.4; 26.1. EI-MS (70 eV): 500 (3), 498 (5), 496 (2, $C_{23}H_{30}Br_2O_2^+$; $M^{+\bullet}$), 419 (54), 417 (55, $[M-Br]^+$), 338 (3, $[M-2Br]+\bullet$), 107 (100, $[HOC_6H_4CH_2]^+$).

1,1′-[Decane-1,10-diylbis(oxy)]bis[4-(bromomethyl)benzene] (**9h**). ^{1}H-NMR (250 MHz, $CDCl_3$): 1.45–1.70 (*m*, 6 CH_2); 1.73–1.91 (*m*, 2 CH_2); 3.95 (*t*, 2 CH_2O); 4.50 (*s*, 2 CH_2Br); 6.85 (*AA′* of *AA′XX′*, ^3J = 8.7, 4 arom. H); 7.33 (*XX′* of *AA′XX′*, ^3J = 8.7, 4 arom. H). ^{13}C-NMR (62.5 MHz, $CDCl_3$): 159.0; 130.2; 129.8; 114.5; 67.9; 34.0; 29.5; 29.3; 29.1; 26.2. EI-MS (70 eV): 514 (2), 512 (5), 510 (3, $C_{24}H_{32}Br_2O_2^+$; $M^{+\bullet}$), 433 (69), 431 (70) $[M-Br]^+$), 352 (7, $[M-2Br]^{+\bullet}$), 107 (100, $[HOC_6H_4CH_2]^+$).

1,1′-[Undecane-1,11-diylbis(oxy)]bis[4-(bromomethyl)benzene] (**9i**). ^{1}H-NMR (300 MHz, $CDCl_3$): 1.44–1.69 (*m*, 7 CH_2); 1.76–1.87 (*m*, 2 CH_2); 3.89 (*t*, 2 CH_2O); 4.43 (*s*, 2 CH_2Br); 6.92 (*AA′* of *AA′XX′*, ^3J = 8.7, 4 arom. H); 7.29 (*XX′* of *AA′XX′*, ^3J = 8.7, 4 arom. H). ^{13}C-NMR (75 MHz, $CDCl_3$): 159.6; 130.8; 130.1; 115.2; 68.5; 34.3; 29.9; 29.8; 29.8; 29.6; 26.4. EI-MS (70 eV): 528 (2), 526 (4), 524 (4, $C_{25}H_{34}Br_2O_2^+$; $M^{+\bullet}$), 447 (45), 445 (46, $[M-Br]^+$), 464 (5, $[M-2Br]^{+\bullet}$), 107 (100, $[HOC_6H_4CH_2]^+$).

1,1′-[Dodecane-1,12-diylbis(oxy)]bis[4-(bromomethyl)benzene] (**9j**). ^{1}H-NMR (300 MHz, $CDCl_3$): 1.28–1.56 (*m*, 8 CH_2); 1.69–1.85 (*m*, 2 CH_2); 3.94 (*t*, 2 CH_2O); 4.49 (*s*, 2 CH_2Br); 6.84 (*AA′* of *AA′XX′*, ^3J = 8.7, 4 arom. H); 7.31 (*XX′* of *AA′XX′*, ^3J = 8.7, 4 arom. H). ^{13}C-NMR (75 MHz, $CDCl_3$): 159.3; 130.4; 129.7; 114.7; 68.0; 34.1; 29.5; 29.4; 29.3; 29.2; 26.0. EI-MS (70 eV): 542 (3), 540 (5), 538 (3, $C_{26}H_{36}Br_2O_2^+$; $M^{+\bullet}$), 461 (49), 459 (48, $[M-Br]^+$), 478 (4, $[M-2Br]^{+\bullet}$), 107 (100, $[HOC_6H_4CH_2]^+$).

Rotaxanes: Protocol A, *General Procedure* [9]. Wheel **3** was stirred in CH_2Cl_2 together with 1 equiv. of the dibromide axle-center piece **9a**–**j**, 2 equiv. of the stopper **2** or **10**, 0.25 equiv. of dibenzo[18]crown-6, and an

excess of K_2CO_3 for 6 days. After evaporation, the rotaxane was purified by CC (CH_2Cl_2/AcOEt gradient 30:1 → 10:1, silica gel (40–63 μ)). The rotaxanes were obtained as colorless wax-like, sometimes oily substances, the melting points of which could not be determined.

Rotaxanes: Protocol B, General Procedure. Wheel **3** was stirred in CH_2Cl_2 together with 1 equiv. of the dibromide axle-center piece **9a–j**, 2 equiv. of the stopper **2** or **10**, 0.5 equiv. of dibenzo[18]crown-6, and an excess of K_2CO_3 for 3 days. During this period, six additional portions of 1 equiv. of **9a–j** and 2 equiv. of the stopper each were added after more or less equidistant time intervals. The rotaxane was purified by CC (see above).

Rotaxane **12a·3**: *Protocol C*, via *Complete Deprotonation prior to Axle Formation*. Stopper **10** was dissolved in CH_2Cl_2 and cooled in an ice bath to 0°. Slowly, 1 equiv. of BuLi in hexanes was added for complete deprotonation. After warming to r.t., wheel **3** was added in an equimolar amount. The generation of the stopper wheel complex $\mathbf{10}^- \cdot \mathbf{3}$ was indicated by the formation of a precipitate which completely dissolves again after addition of 1 equiv. of [15]crown-5. Addition of the axle-center piece and stirring for 24 h yielded the rotaxane and free axle, which were purified by CC (see above).

Rotaxane **12a·3**: *Protocol D*, via *Complete Deprotonation of the Stopper and Addition of $AgNO_3$ as a Bromide Scavenger*. The stopper wheel complex $\mathbf{10}^- \cdot \mathbf{3}$ was generated as described in *Protocol C*. After addition of the axle-center piece, 2 equiv. of $AgNO_3$ (or $AgBF_4$) was added. The silver salt was hardly soluble in CH_2Cl_2, and sonication for 15 to 30 min was applied to increase the reactive surface. Immediately, AgBr precipitated. After completion of the reaction, the precipitate was filtered off and the filtrate purified as indicated above.

*[2]{1,1′-[Propane-1,3-diylbis(oxy)]bis[4-{[3,5-di(*tert*-butyl)phenoxy]methyl}benzene]}-{11′-(*tert*-butyl)-5′,17′,23′,35′,38′,40′,43′,45′-octamethyldispiro[cyclohexane-1,2′-[7,15,25,33]tetraazaheptacyclo[32.2.2.2^{3,6}.2^{16,19}.2^{21,24}.1^{9,13}.1^{27,31}]hexatetraconta[3,5,9,11,13(44),16,18,21,23,27,29,31,(39),34,36,37,40,42,45]octadecaene-20′,1″-cyclohexane]-8′,14′,26′,32′-tetrone}rotaxane* (**12a·3**): R_f 0.18 (CH_2Cl_2/AcOEt 30:1). Yield 3% (*A*), 23% (*B*). ^{1}H-NMR (400 MHz,$C_2D_2Cl_4$): 1.25 (*s*, 4 ^{t}Bu (axle)); 1.44 (*s*, 1 ^{t}Bu (wheel)); 1.60 (br., 2 CH_2 (chx)); 1.68 (*q*, ^3J = 6.0, 2 H, CH_2 (axle)); 1.74 (br., 4 CH_2 (chx)); 1.98 (*s*, 4 Me (wheel)); 2.00 (*s*, 4 Me (wheel)); 2.41 (br., 4 CH_2 (chx)); 3.85 (*t*, ^3J = 6.0, 2 CH_2O (axle)); 4.59 (*s*, 2 CH_2O (axle)); 6.14 (*AA′*of *AA′XX′*, ^3J = 8.5, 4 arom. H (axle)); 6.54 (*XX′* of *AA′XX′*, ^3J = 8.5, 4 arom. H (axle)); 6.66 (br. *s*, 4 NH); 7.04 (*s*, 2 arom. H (axle)); 7.08 (*s*, 4 arom. H (wheel)); 7.10 (*s*, 4 arom. H (wheel)); 7.32 (*s*, 4 arom. H (axle)); 7.66 (*s*, 1 arom. H (wheel)); 7.68 (*t*, ^3J = 7.7, 1 arom. H (wheel)); 7.80 (*s*, 1 arom. H (wheel)); 8.17 (*d*, ^3J = 7.7, 2 arom. H (wheel)); 8.21 (*s*, 2 arom. H (wheel)). ^{13}C-NMR (100 MHz, $C_2D_2Cl_4$): 18.6; 22.9; 28.5; 31.0; 31.2; 31.8; 34.6; 35.0; 35.4; 45.3; 64.7; 69.7; 108.5; 114.4; 114.5; 114.6; 115.7; 126.6; 126.7; 128.5; 128.9; 129.1; 130.9; 131.1; 134.2; 134.4; 134.9; 135.0; 148.7; 152.3; 157.6; 157.8; 164.8; 165.2. MALDI-TOF-MS 1662.9 (67, $C_{109}H_{132}KN_4O_8^+$, $[M+K^+]$), 1646.9 (100, $[M+Na]^+$), 998.7 (27, $[wheel+K]^+$), 982.8 (65, $[wheel+Na]^+$), 960.8 (66, $[wheel+H]^+$).

*[2]{1,1′-[Butane-1,4-diylbis(oxy)]bis[4-{[3,5-di(*tert*-butyl)phenoxy]methyl]benzene]}-{11′-(*tert*-butyl)-5′,17′,23′,35′,38′,40′,43′,45′-octamethyldispiro[cyclohexane-1,2′-[7,15,25,33]tetraazaheptacyclo[32.2.2.2^{3,6}.2^{16,19}.2^{21,24}.1^{9,13}.1^{27,31}]hexatetraconta[3,5,9,11,13(44),16,18,21,23,27,29,31,(39),34,36,37,40,42,45]octadecaene-20′,1″-cyclohexane]-8′,14′,26′,32′-tetrone}rotaxane* (**12b·3**): R_f 0.20 (CH_2Cl_2/AcOEt 30:1). Yield 5% (*A*), 21% (*B*). ^{1}H-NMR (400 MHz, $C_2D_2Cl_4$): 1.25 (*s*, 4 ^{t}Bu (axle)); 1.44 (*s*, 1 ^{t}Bu (wheel)); 1.61 (br., 2 CH_2 (chx)); 1.65–1.84 (*m*, 6 CH_2 (chx, axle)); 1.98 (*s*, 4 Me (wheel)); 2.01 (*s*, 4 Me (wheel)); 2.42 (br., 4 CH_2 (chx)); 3.75 (*t*, ^3J = 6.9, 2 CH_2O (axle)); 4.60 (*s*, 2 CH_2O (axle)); 6.15 (*AA′* of *AA′XX′*, ^3J = 8.5, 4 arom. H (axle)); 6.56 (*XX′* of *AA′XX′*, ^3J = 8.5, 4 arom. H (axle)); 6.66 (br. *s*, 4 NH); 7.04 (*s*, 2 arom. H (axle)); 7.09 (*s*, 4 arom. H (wheel)); 7.10 (*s*, 4 arom. H (wheel)); 7.29 (*s*, 4 arom. H (axle)); 7.72 (*s*, 1 arom. H (wheel)); 7.73 (*t*, ^3J = 7.7, 1 arom. H (wheel)); 7.85 (*s*, 1 arom. H (wheel)); 8.21 (*d*, ^3J = 7.7, 2 arom. H (wheel)); 8.23 (*s*, 2 arom. H (wheel)). ^{13}C-NMR (100 MHz, $C_2D_2Cl_4$): 18.6; 22.5; 25.7; 29.5; 31.0; 31.2; 31.8; 34.6; 35.0; 35.8; 45.3; 64.7; 67.4; 108.6; 114.3; 114.4; 114.6; 115.7; 126.5; 126.7; 128.5; 128.7; 129.1; 130.9; 131.1; 134.1; 134.3; 135.0; 152.3; 157.6; 158.0; 164.8; 165.2. MALDI-TOF-MS: 1678.8 (12, $C_{110}H_{134}KN_4O_8^+$ $[M+K^+]$), 1662.8 (87, $[M+Na]^+$), 999.4 (15, $[wheel+K]^+$), 983.4 (100, $[wheel+Na]^+$), 961.4 (65, $[wheel+H]^+$).

*[2]{1,1′-[Pentane-1,5-diylbis(oxy)]bis[4-{[3,5-di(*tert*-butyl)phenoxy]methyl}benzene]}-{11′-(*tert*-butyl)-5′,17′,23′,35′,38′,40′,43′,45′-octamethyldispiro[cyclohexane-1,2′-[7,15,25,33]tetraazaheptacyclo[32.2.2.2^{3,6}.2^{16,19}.2^{21,24,1}9.^{13}.1^{27,31}]hexatetraconta[3,5,9,11,13(44),16,18,21,23,27,29,31(39),34,36,37,40,42,45]octadecaene-20′,1″-cyclohexane]-8′,14′,26′,32′-tetrone}rotaxane* (**12c·3**): R_f 0.21 (CH_2Cl_2/AcOEt 30:1). Yield 5% (*A*), 19% (*B*). ^{1}H-NMR (400 MHz, $C_2D_2Cl_4$): 1.20–1.30 (*m*, 1 CH_2 (axle)); 1.25 (*s*, 4 ^{t}Bu (axle)); 1.43 (*s*, 1 ^{t}Bu (wheel)); 1.62 (br., 2 CH_2 (chx)); 1.65–1.84 (*m*, 6 CH_2 (chx, axle)); 1.98 (*s*, 4 Me (wheel)); 2.01 (*s*, 4 Me (wheel)); 2.41 (br., 4 CH_2 (chx)); 3.72 (*t*, ^3J = 6.2, 2 CH_2O (axle)); 4.60 (*s*, 2 CH_2O (axle)); 6.17 (*AA′* of *AA′XX′*, ^3J = 8.5, 4 arom. H (axle)); 6.46 (*XX′* of *AA′XX′*, ^3J = 8.5, 4 arom. H (axle)); 6.67 (br. *s*, 4 NH); 7.05 (*s*, 2 arom. H (axle)); 7.09 (*s*, 4 arom. H (wheel)); 7.10 (*s*, 4 arom. H (wheel)); 7.35 (*s*, 4 arom. H (axle)); 7.69 (*s*, 1 arom. H (wheel)); 7.70 (*t*, ^3J = 7.7, 1 arom. H (wheel)); 7.84 (*s*, 1 arom. H (wheel)); 8.20 (*d*, ^3J = 7.7, 2 arom. H (wheel)); 8.22

(*s*, 2 arom. H (wheel)). ^{13}C-NMR (100 MHz, $C_2D_2Cl_4$): 18.6; 22.9; 28.5; 31.0; 31.1; 31.2; 31.8; 34.7; 35.0; 35.4; 45.3; 64.7; 69.7; 108.6; 114.4; 114.5; 114.6; 115.7; 126.5; 126.7; 128.5; 128.9; 129.1; 130.9; 131.1; 134.2; 134.3; 134.9; 135.0; 148.8; 152.3; 157.6; 158.1; 158.4; 164.7; 165.1. MALDI-TOF-MS: 1692.0 (42, $C_{111}H_{136}KN_4O_8^+$ [M + K^+]), 1676.0 (100, [M + $Na]^+$), 99.2 (20, [wheel + $K]^+$), 983.2 (88, [wheel + $Na]^+$), 961.2 (91, [weel + $H]^+$).

[2]{1,1′-[Hexane-1,6-diylbis(oxy)]bis[4-{[3,5-di(tert-*butyl)phenoxy]methyl}benzene]}-{11′-*(tert-*butyl)-5′,17′,23′,35′,38′,40′,43′,45′-octamethyldispiro[cyclohexane-1,2′-[7,15,25,33]tetraazaheptacyclo[32.2.2.2^{3,6}.2^{16,19}.2^{21,24}.1^{9,13}.1^{27,31}]hexatetraconta[3,5,9,11,13(44),16,18,21,23,27,29,31(39),34,36,37,40,42,45]octadecaene-20′,1″-cyclohexane]-8′,14′,26′,32′-tetrone}rotaxane* **12d**·**3**): R_f 0.21 (CH_2Cl_2/AcOEt 30:1): Yield 3% (*A*), 16% (*B*). ^{1}H-NMR (400 MHz, $C_2D_2Cl_4$): 1.20–1.30 (*m*, 2 CH_2 (axle)); 1.25 (*s*, 4 ^{t}Bu (axle)); 1.44 (*s*, 1 ^{t}Bu (wheel)); 1.62 (br., 2 CH_2 (chx)); 1.65–1.84 (*m*, 6 CH_2 (chx, axle)); 1.98 (*s*, 4 Me (wheel)); 2.01 (*s*, 4 Me (wheel)); 2.42 (br., 4 CH_2 (chx)); 3.73 (*t*, ^3J = 6.5, 2 CH_2O (axle)); 4.60 (*s*, 2 CH_2O (axle)); 6.17 (*AA′* of *AA′XX′*, ^3J = 8.3, 4 arom. H (axle)); 6.45 (*XX′* of *AA′XX′*, ^3J = 8.3, 4 arom. H (axle)); 6.67 (br. *s*, 4 NH); 7.05 (*s*, 2 arom. H (axle)); 7.09 (*s*, 4 arom. H (wheel)); 7.10 (*s*, 4 arom. H (wheel)); 7.36 (*s*, 4 arom. H (axle)); 7.69 (*s*, 1 arom. H (wheel)); 7.71 (*t*, ^3J = 7.8, 1 arom. H (wheel)); 7.84 (*s*, 1 arom. H (wheel)); 8.22 (*d*, ^3J = 7.8, 2 arom. H (wheel)); 8.23 (*s*, 2 arom. H (wheel)). ^{13}C-NMR (100 MHz, $C_2D_2Cl_4$): 18.6; 22.9; 25.6; 28.5; 29.5; 31.0; 31.1; 31.2; 31.8; 34.7; 35.0; 35.4; 45.3; 67.7; 68.3; 108.6; 114.2; 114.5; 114.6; 115.7; 126.5; 126.7; 128.5; 128.8; 129.1; 130.9; 131.0; 134.1; 134.3; 135.0; 152.3; 157.6; 158.2; 158.4; 164.7; 165.1. MALDI-TOF-MS: 1706.1 (78, $C_{112}H_{138}KN_4O_8^+$ [M + K^+]), 1690.0 (100, [M + $Na]^+$), 998.8 (61, [wheel + $K]^+$), 982.8 (97, [wheel + $Na]^+$), 960.8 (71, [wheel + $H]^+$).

[2]{(1,1′-[Heptane-1,7-diylbis(oxy)]bis[4-{[3,5-di(tert-*butyl)phenoxy]methyl}benzene]}-{11′-*(tert-*butyl)-5′,17′,23′,35′,38′,40′,43′,45′-octamethyldispiro[cyclohexane-1,2′-[7,15,25,33]tetraazaheptacyclo[32.2.2.2^{3,6}.2^{16,19}.2^{21,24}.1^{9,13}.1^{27,31}]hexatetraconta[3,5,9,11,13(44),16,18,21,23,27,29,31(39),34,36,37,40,42,45]octadecaene-20′,1″-cyclohexane]-8′,14′,26′,32′-tetrone}rotaxane* (**12e**·**3**): R_f 0.23 (CH_2Cl_2/AcOEt 30:1). Yield 5% (*A*), 22% (*B*). ^{1}H-NMR (400 MHz, $C_2D_2Cl_4$): 1.20–1.30 (*m*, 3 CH_2 (axle)); 1.25 (*s*, 4 ^{t}Bu (axle)); 1.44 (*s*, 1 ^{t}Bu (wheel)); 1.63 (br., 2 CH_2 (chx, axle)); 1.65–1.84 (*m*, 6 CH_2 (chx)); 1.98 (*s*, 4 Me (wheel)); 2.01 (*s*, 4 Me (wheel)); 2.42 (br., 4 CH_2 (chx)); 3.73 (*t*, ^3J = 6.8, 2 CH_2O (axle)); 4.60 (*s*, 2 CH_2O (axle)); 6.17 (*AA′* of *AA′XX′*, ^3J = 8.2, 4 arom. H (axle)); 6.55 (*XX′* of *AA′XX′*, ^3J = 8.2, 4 arom. H (axle)); 6.67 (br. *s*, 4 NH); 7.05 (*s*, 2 arom. H (axle)); 7.08 (*s*, 4 arom. H (wheel)); 7.11 (*s*, 4 arom. H (wheel)); 7.36 (*s*, 4 arom. H (axle)); 7.69 (*s*, 1 arom. H (wheel)); 7.71 (*t*, J = 7.5, 1 arom. H (wheel)); 7.84 (*s*, 1 arom. H (wheel)); 8.22 (*d*, ^3J = 7.5, 2 arom. H (wheel)); 8.23 (*s*, 2 arom. H (wheel)). ^{13}C-NMR (100 MHz, $C_2D_2Cl_4$): 18.6; 22.9; 25.7; 25.8; 28.9; 29.5; 31.0; 31.1; 31.2; 31.8; 34.6; 35.0; 35.8; 45.3; 64.7; 68.5; 108.6; 114.4; 114.6; 114.7; 115.7; 126.5; 126.7; 128.5; 128.8; 129.1; 130.9; 131.0; 134.1; 134.3; 135.0; 152.3; 157.6; 158.2; 164.7, 165.1. MALDI-TOF-MS: 1720.3 (99, $C_{113}H_{140}KN_4O_8^+$ [M + $K]^+$), 1704.3 (100, [M + $Na]^+$), 999.1 (73, [wheel + $K]^+$), 983.1 (84, [wheel + $Na]^+$), 961.1 (72, [wheel + $H]^+$).

[2]{1,1′-[Octane-1,8-diylbis(oxy)]bis[4-{[3,5-di(tert-*butyl)phenoxy]methyl}benzene]}-{11′-*(tert-*butyl)-5′,17′,23′,35′,38′,40′,43′,45′-octamethyldispiro[cyclohexane-1,2′-[7,15,25,33]tetraazaheptacyclo[32.2.2.2^{3,6}.2^{16,19}.2^{21,24}.1^{9,13}.1^{27,31}]hexatetraconta[3,5,9,11,13(44),16,18,21,23,27,29,31(39),34,36,37,40,42,45]octadecaene-20′,1″-cyclohexane]-8′,14′,26′,32′-tetrone}rotaxane* (**12f**·**3**): R_f 0.24 (CH_2Cl_2/AcOEt 30:1). Yield 4% (*A*), 22% (*B*). ^{1}H-NMR (400 MHz, $C_2D_2Cl_4$): 1.20–1.30 (*m*, 4 CH_2 (axle)); 1.25 (*s*, 4 ^{t}Bu(axle)); 1.44 (*s*, 1 ^{t}Bu (wheel)); 1.60–1.84 (*m*, 4 CH_2 (chx, axle)); 1.97 (*s*, 4 Me (wheel)); 2.01 (*s*, 4 Me (wheel)); 2.42 (br. 4 CH_2 (chx)); 3.73 (*t*, ^3J = 6.5, 2 CH_2O (axle)); 4.60 (*s*, 2 CH_2O (axle)); 6.17 (*AA′* of *AA′XX′*, ^3J = 8.0, 4 arom. H (axle)); 6.55 (*XX′* of *AA′XX′*, ^3J = 8.0, 4 arom. H (axle)); 6.67 (br. *s*, 4 NH); 7.05 (*s*, 2 arom. H (axle)); 7.08 (*s*, 4 arom. H (wheel)); 7.10 (*s*, 4 arom. H (wheel)); 7.37 (*s*, 4 arom. H (axle)); 7.69 (*s*, 1 arom. H (wheel)); 7.71 (*t*, ^3J = 7.6, 1 arom. H (wheel)); 7.84 (*s*, 1 arom. H (wheel)); 8.22 (*d*, ^3J = 7.6, 2 arom. H (wheel)); 8.23 (*s*, 2 arom. H (wheel)). ^{13}C-NMR (100 MHz, $C_2D_2Cl_4$): 18.6; 22.9; 25.7; 29.0; 29.1; 31.0; 31.1; 31.2; 31.3; 31.8; 34.6; 35.0; 35.4; 45.3; 67.9; 68.6; 108.6; 114.3; 114.7; 115.7; 126.5; 126.7; 128.7; 129.1; 129.3; 130.9; 131.0; 134.1; 134.3; 135.0; 148.8; 152.3; 157.6; 158.3; 164.7; 165.1. MALDI-TOF-MS: 1734.3 (52, $C_{114}H_{142}KN_4O_8^+$ [M + K^+]), 1718.3 (100, [M + $Na]^+$), 982.9 (85, [wheel + $Na]^+$), 960.9 (79, [wheel + $H]^+$).

[2]{1,1′-[Nonane-1,9-diylbis(oxy)]bis[4-{[3,5-di(tert-*butyl)phenoxy]methyl}benzene]}-{11′-*(tert-*butyl)-5′,17′,23′,35′,38′,40′,43′,45′-octamethyldispiro[cyclohexane-1,2′-[7,15,25,33]tetraazaheptacyclo[32.2.2.2^{3,6}.2^{16,19}.2^{21,24}.1^{9,13}.1^{27,31}]hexatetraconta[3,5,9,11,13(44),16,18,21,23,27,29,31(39),34,36,37,40,42,45]octadecaene-20′,1″-cyclohexane]-8′,14′,26′,32′-tetrone}rotaxane* (**12g**·**3**): R_f 0.25 (CH_2Cl_2/AcOEt 30:1). Yield 2% (*A*), 17% (*B*). ^{1}H-NMR (400 MHz, $C_2D_2Cl_4$): 1.20–1.30 (*m*, 5 CH_2 (axle)); 1.25 (*s*, 4 ^{t}Bu (axle)); 1.44 (*s*, 1 ^{t}Bu (wheel)); 1.60–1.84 (*m*, 8 CH_2 (chx, axle)); 1.97 (*s*, 4 Me (wheel)); 2.01 (*s*, 4 Me (wheel)); 2.42 (br., 4 CH_2 (chx)); 3.74 (*t*, ^3J = 6.5, 2 CH_2 (axle)); 4.61 (*s*, 2 CH_2O (axle)); 6.17 (*AA′* of *AA′XX′*, ^3J = 7.8, 4 arom. H (axle)); 6.55 (*XX′* of *AA′XX′*, ^3J = 7.8, 4 arom. H (axle)); 6.67 (br. *s*, 4 NH); 7.05 (*s*, 2 arom. H (axle)); 7.08 (*s*, 4 arom. H (wheel)); 7.10 (*s*, 4 arom. H (wheel)); 7.37 (*s*, 4 arom. H (axle)); 7.69 (*s*, 1 arom. H (wheel)); 7.71 (*t*, ^3J = 7.7, 1 arom. H (wheel)); 7.84 (*s*, 1 arom. H (wheel)); 8.22 (*d*, ^3J = 7.7, 2 arom. H (wheel)); 8.23 (*s*, 2 arom. H (wheel)).

^{13}C-NMR (100 MHz, $C_2D_2Cl_4$): 18.6; 22.9; 25.8; 29.0; 29.1; 29.3; 31.0; 31.1; 31.2; 31.3; 31.8; 34.6; 35.0; 35.4; 45.3; 68.6; 70.1; 108.6; 114.7; 115.7; 126.5; 126.7; 128.7; 129.1; 130.9; 131.0; 132.1; 134.1; 134.3; 135.0; 148.8; 152.3; 157.6; 158.3; 164.7; 165.1. MALDI-TOF-MS: 1748.3 (38, $C_{115}H_{114}KN_4O_8^+$ [$M+K^+$]), 1732.3 (100, [$M+Na]^+$), 983.1 (99, [wheel + $Na]^+$), 961.0 (92, [wheel + $H]^+$).

[2]{1,1′-[Decane-1,10-diylbis(oxy)]bis[4-{[3,5-di(tert-*butyl)phenoxy]methyl}benzene]}-{11′-(*tert-*butyl)-5′,17′,23′,35′,38′,40′,43′,45′-octamethyldispiro[cyclohexane-1,2′-[7,15,25,33]tetraazaheptacyclo[32.2.2.2$^{3.6}$.2$^{16.19}$.2$^{1.24}$.1$^{9.13}$.1$^{27.31}$]hexatetraconta[3,5,9,11,13(44),16,18,21,23,27,29,31(39),34,36,37,40,42,45]octadecaene-20′,1″-cyclohexane]-8′,14′,26′,32′-tetrone}rotaxane* (**12h**·**3**): R_f 0.26 (CH_2Cl_2/AcOEt 30:1). Yield 4% (*A*), 21% (*B*). ^{1}H-NMR (400 MHz, $C_2D_2Cl_4$): 1.20–1.30 (*m*, 4 Me (axle)); 1.25 (*s*, 4 ^{t}Bu (axle)); 1.44 (*s*, 1 ^{t}Bu (wheel)); 1.60–1.84 (*m*, 8 CH_2 (chx, axle)); 1.97 (*s*, 4 Me (wheel)); 2.00 (*s*, 4 Me (wheel)); 2.42 (br. 4 CH_2 (chx)); 3.74 (*t*, ^3J = 6.6, 2 CH_2O (axle)); 4.61 (*s*, 2 CH_2O (axle)); 6.17 (*AA′* of *AA′XX′*, ^3J = 7.4, 4 arom. H (axle)); 6.55 (*XX′* of *AA′XX′*, ^3J = 7.4, 4 arom. H (axle)); 6.67 (br. *s*, 4 NH); 7.05 (*s*, 2 arom. H (axle)); 7.08 (*s*, 4 arom. H (wheel)); 7.10 (*s*, 4 arom. H (wheel)); 7.37 (*s*, 4 arom. H (axle)); 7.69 (*s*, 1 arom. H (wheel)); 7.71 (*t*, ^3J = 7.7, 1 arom. H (wheel)); 7.85 (*s*, 1 arom. H (wheel)); 8.22 (*d*, ^3J = 7.7, 2 arom. H (wheel)); 8.23 (*s*, 2 arom. H (wheel)). ^{13}C-NMR (100 MHz, $C_2D_2Cl_4$): 18.6; 22.9; 25.8; 26.2; 29.0; 29.1; 29.3; 31.0; 31.1; 31.3; 31.8; 34.6; 35.0; 35.4; 45.3; 68.6, 70.1; 108.7; 114.7; 115.7;126.5; 126.7; 128.7; 129.1; 130.9; 131.0; 132.1; 134.1; 134.3; 135.0; 148.7; 152.3; 153.9; 157.6; 158.3; 164.7; 165.1. MALDI-TOF-MS: 1762.2 (30, $C_{116}H_{146}KN_4O_8^+$ [$M+K^+$]), 1746.2 (100, [$M+Na]^+$), 983.2 (54, [wheel + $Na]^+$), 960.5 (39, [wheel + $H]^+$).

[2]{1,1′-[Undecane-1,11-diylbis(oxy)]bis[4-{[3,5-di(tert-*butyl)phenoxy]methyl}benzene]}-{11′-(*tert-*butyl)-5′,17′,23′,35′,38′,40′,43′,45′-octamethyldispiro[cyclohexane-1,2′-[7,15,25,33]tetraazaheptacyclo[32.2.2.2.$^{3.6}$.2$^{16.19}$.2$^{21.24}$.1$^{9.13}$.1$^{27.31}$]hexatetraconta[3,5,9,11,13(44),16,18,21,23,27,29,31(39),34,36,37,40,42,45]octadecaene-20′,1″-cyclohexane]-8′,14′,26′,32′-tetrone}rotaxane* (**12i**·**3**): R_f 0.28 (CH_2Cl_2/AcOEt 30:1). Yield 5% (*A*), 24% (*B*). ^{1}H-NMR (400 MHz, $C_2D_2Cl_4$): 1.20–1.30 (*m*, 7 CH_2 (axle)); 1.25 (*s*, 4 ^{t}Bu (axle)); 1.44 (*s*, 1 ^{t}Bu (wheel)); 1.60–1.84 (*m*, 8 CH_2 (chx, axle)); 1.97 (*s*, 4 Me (wheel)); 2.00 (*s*, 4 Me (wheel)); 2.42 (br. 4 CH_2 (chx)); 3.74 (*t*, ^3J = 6.5, 2 CH_2O (axle)); 4.61 (*s*, 2 CH_2O (axle)); 6.17 (*AA′* of *AA′XX′*, ^3J = 7.8, 4 arom. H (axle)); 6.55 (*XX′* of *AA′XX′*, ^3J = 7.8, 4 arom. H (axle)); 6.67 (br. *s*, 4 NH); 7.05 (*s*, 2 arom. H (axle)); 7.08 (*s*, 4 arom. H (wheel)); 7.10 (*s*, 4 arom. H (wheel)); 7.37 (*s*, 4 arom. H (axle)); 7.69 (*s*, 1 arom. H (wheel)); 7.72 (*t*, ^3J = 7.7, 1 arom. H (wheel)); 7.84 (*s*, 1 arom. H (wheel)); 8.22 (*d*, ^3J = 7.7, 2 arom. H (wheel)); 8.23 (*s*, 2 arom. H (wheel)). ^{13}C-NMR (100 MHz, $C_2D_2Cl_4$): 18.6; 22.9; 25.8; 29.0; 29.1; 29.4; 29.5; 31.0; 31.1; 31.2; 31.3; 31.8; 34.6; 35.0; 35.4; 35.8; 45.3; 68.7; 70.1; 108.6; 114.5; 115.7; 126.5; 126.7; 128.7; 129.1; 130.9; 131.0; 132.1; 134.1; 134.3; 135.0; 148.8; 152.3; 157.6; 158.3; 164.7; 165.1. MALDI-TOF-MS: 1776.3 (22, $C_{117}H_{148}KN_4O_8^+$ [$M+K^+$]), 1760.3 (100, [$M+Na]^+$), 1737.3 (3, [$M+H]^+$), 983.2 (82, [wheel + $Na]^+$), 960.5 (96, [wheel + $H]^+$).

[2]{1,1′[Dodecane-1,12-diylbis(oxy)]bis[4-{[3,5-di(tert-*butyl)phenoxy]methyl}benzene]}-{11′-(*tert-*butyl)5′,17′,23′,35′,38′,40′,43′,45′-octamethyldispiro[cyclohexane-1,2′-[7,15,25,33]tetraazaheptacyclo[32.2.2.2$^{3.6.2}$16.19.2$^{21.24.19.13}$.1$^{27.31}$]hexatetraconta[3,5,9,11,13(44),16,18,21,23,27,29,31(39),34,36,37,40,42,45]octadecaene-20′,1″-cyclohexane]-8′,14′,26′,32′-tetrone}rotaxane* (**12j**·**3**). R_f 0.29 (CH_2Cl_2/AcOEt 30:1). Yield 3% (*A*), 19% (*B*). ^{1}H-NMR (400 MHz, $C_2D_2Cl_4$): 1.20–1.30 (*m*, 8 CH_2 (axle)); 1.25 (*s*, 4 ^{t}Bu (axle)); 1.44 (*s*, 1 ^{t}Bu (wheel)); 1.60–1.84 (*m*, 8 CH_2 (chx, axle)); 1.98 (*s*, 4 Me (wheel)); 2.00 (*s*, 4 Me (wheel)); 2.43 (br., 4 CH_2 (chx)); 3.74 (*t*, ^3J = 6.6, 2 CH_2O (axle)); 4.61 (*s*, 2 CH_2O (axle)); 6.17 (*AA′* of *AA′XX′*, ^3J = 7.8, 4 arom. H (axle)); 6.54 (*XX′* of *AA′XX′*, ^3J = 7.8, 4 arom. H (axle)); 6.67 (br. *s*, 4 NH); 7.05 (*s*, 2 arom. H (acle)); 7.08 (*s*, 4 arom. H (wheel)); 7.10 (*s*, 4 arom. H (wheel)); 7.37 (*s*, 4 arom. H (axle)); 7.69 (*s*, 1 arom. H (wheel)); 7.72 (*t*, ^3J = 7.8, 1 arom. H (wheel)); 7.84 (*s*, 1 arom. H (wheel)); 8.22 (*d*, ^3J = 7.8, 2 arom. H (wheel)); 8.23 (*s*, 2 arom. H (wheel)). ^{13}C-NMR (100 MHz, $C_2D_2Cl_4$): 18.5; 22.9; 25.8; 29.0; 29.2; 29.3; 29.4; 31.0; 31.1; 31.2; 31.3; 34.6; 35.0; 35.4; 45.3; 68.6; 70.1; 108.7; 114.7; 115.7; 126.5; 126.7; 128.7; 129.1; 130.9; 131.0; 132.1; 134.1; 134.3; 135.0; 152.3; 157.6; 158.3; 164.7; 165.1. MALDI-TOF-MS: 1790.0 (13, $C_{118}H_{150}KN_4O_8^+$ [$M+K^+$]), 1773.9 (95, [$M+Na]^+$), 1750.9 (5, [$M+H]^+$), 983.2 (83, [wheel + $Na]^+$), 960.5 (100, [wheel + $H]^+$).

[2]{1,1′-[Octane-1,8-diylbis(oxy)]bis[4-{[4-(triphenylmethyl)phenoxy]methyl}benzene]}-{11′-(*tert-*butyl)-5′,17′,23′,35′,38′,40′,43′,45′-oxtamethyldispiro[cyclohexane-1,2′-[7,15,25,33]tetraazaheptacyclo[32.2.2.2.$^{3.6}$.2$^{16.19}$.2$^{21.24}$.1$^{9.13}$.1$^{27.31}$]hexatetraconta[3,5,9,11,13(44),16,18,21,23,27,29,31(39),34,36,37,40,42,45]octadecaene-20′,1″-cyclohexane]-8′,14′,26′,32′-tetrone}rotaxane* **14f**·**3**: R_f 0.29 (CH_2Cl_2/AcOEt 30:1). Yield 35% (*A*). ^{1}H-NMR (400 MHz, $CDCl_3$): 1.20–1.40 (*m*, 4 CH_2 (axle)); 1.36 (*s*, 1 ^{t}Bu (wheel)); 1.50–1.73 (*m*, 8 CH_2 (chx, axle)); 1.97 (*s*, 4 Me (wheel)); 1.99 (*s*, 4 Me (wheel)); 2.34 (br. 4 CH_2 (chx)); 3.72 (*t*, ^3J = 6.5, 2 CH_2O (axle)); 4.61 (*s*, 2 CH_2O (axle)); 6.17 (*AA′* of *AA′XX′*, ^3J = 7.8, 4 arom. H (axle)); 6.55 (*XX′* of *AA′XX′*, ^3J = 7.8, 4 arom. H (axle)); 6.84 (br. *s*, 4 NH); 7.01–7.07 (*m*, 10 arom. H (axle, wheel)); 7.10–7.25 (*m*, 6 Ph); 7.60 (*s*, 1 arom. H (wheel)); 7.70 (*t*, ^3J = 7.4, 1 arom. H (wheel)); 7.80 (*s*, 1 arom. H (wheel)); 8.19 (*d*, ^3J = 7.4, 2 arom. H (wheel)); 8.22 (*s*, 2 arom. H (wheel)). ^{13}C-NMR (100 MHz, $CDCl_3$): 14.2; 18.8; 21.0; 23.0; 26.0; 29.3; 31.2; 35.4; 35.8; 45.4;

60.4; 64.3; 68.7; 70.2; 113.5; 115.0; 117.2; 121.4; 123.9; 126.0; 126.8; 126.9; 127.0; 128.7; 129.1; 129.3; 131.0; 132.1; 132.4; 134.7; 135.0; 140.1; 146.8; 148.9; 154.3; 156.2; 158.6; 164.9; 165.4. MALDI-TOF-MS: 1995.2 (35, $C_{137}H_{140}KN_4O_8^+$ $[M+K^+]$), 1978.2 (100, $[M+Na]^+$), 960.5 (98, [wheel + H]$^+$).

Free Axles. The anal. data of **12c**, which is formed as the undesired major product in the reaction of $\mathbf{10}^- \cdot \mathbf{3}$ and **9c**, is given as representative for the other free axles formed in the rotaxane synthesis.

*1,1′-[Pentane-1,5-diylbis(oxy)]bis[4-{[3,5-di(*tert*-butyl)phenoxy]methyl}benzene]* (**12c**). ^{1}H-NMR (400 MHz, $CDCl_3$): 1.24 (*s*, 4 *t*Bu); 1.60 (*q*, $^3J = 6.5$, 1 CH_2); 1.78 ('*q*', $^3J = 6.5$, 4 H); 3.93 (*t*, $^3J = 6.5$, 2 CH_2O); 4.90 (*s*, 2 C_{H2}OAr), 6.76 (*s*, 4 arom. H (stopper)); 6.83 (*AA′* of *AA′XX′*, $^3J = 8.7$, 4 arom. H); 6.96 (*s*, 2 arom. H (stopper)); 7.29 (*XX′* of *AA′XX′*, $^3J = 8.7$, 4 arom. H. ^{13}C-NMR (100 MHz, $CDCl_3$): 159.0; 158.6; 152.2; 129.5; 129.4; 115.1; 114.7; 109.2; 69.8; 67.9; 35.0; 31.5; 29.1; 22.8. FAB-MS: 691 (15, $C_{47}H_{63}O_4^+$ $[M-H^+]$), 487 (100, $[M - OC_6H_3 - t Bu_2]^+$. MALDI-TOF-MS: 731 (29, $C_{47}H_{64}KO_4^+$ $[M+K^+]$), 715 (72, $[M+Na]^+$), 691 (8, $[M-H]^+$), 467 (100, $[M - OC_6H_3 - {}^t Bu_2]^+$).

REFERENCES

[1] G. Schill, 'Catenanes, Rotaxanes and Knots', Academic Press, New York, 1971; C. O. Dietrich-Buchecker, J.-P. Sauvage, *Chem. Rev.* **1987**, *87*, 795; J.-P. Sauvage, *Acc. Chem. Res.* **1990**, *23*, 319; S. Anderson, H. L. Anderson, J. K. M. Sanders, *Acc. Chem. Res.* **1993**, *26*, 469; R. Hoss, F. Vögtle, *Angew. Chem.* **1994**, *106*, 389; *Angew. Chem., Int. Ed.* **1994**, *33*, 375; D. A. Amabilino, J. F. Stoddart, *Chem. Rev.* **1995**, *95*, 2725; J.-C. Chambron, C. O. Dietrich-Buchecker, V. Heitz, J.-F. Nierengarten, J.-P. Sauvage, C. Pascard, J. Guilhem, *Pure Appl. Chem.* **1995**, *67*, 233; R. Jäger, F. Vögtle, *Angew. Chem., Int. Ed.* **1997**, *36*, 931; S. A. Nepogodiev, J. F. Stoddart, *Chem. Rev.* **1998**, *98*, 1959; F. M. Raymo, J. F. Stoddart, *Chem. Rev.* **1999**, *99*, 1043; 'Molecular Catenanes, Rotaxanes, and Knots', Eds. J. P. Sauvage and C. Dietrich-Buchecker, Wiley-VCH, Weinheim, 1999; C. A. Schalley, K. Beizai, F. Vögtle, *Acc. Chem. Res.* **2001**, *34*, 465.

[2] D. H. Busch, N. A. Stephensen, *Coord. Chem. Rev.* **1990**, *100*, 119; R. Cacciapaglia, L. Mandolini, *Chem. Soc. Rev.* **1993**, *22*, 221; N. V. Gerbeleu, V. B. Arion, J. Burgess, 'Template Synthesis of Macrocyclic Compounds', Wiley-VCH, Weinheim, 1999; 'Templated Organic Synthesis', Eds. F. Diederich and P. J. Stang, Wiley-VCH, Weinheim, 2000; T. J. Hubin, D. H. Busch, *Coord. Chem. Rev.* **2000**, *200–202*, 5.

[3] C. O. Dietrich-Buchecker, J.-P. Sauvage, J.-P. Kintzinger, *Tetrahedron Lett.* **1983**, *24*, 5095; C. O. Dietrich-Buchecker, J.-P. Sauvage, J.-M. Kern, *J. Am. Chem. Soc.* **1984**, *106*, 3043; M. Cesario, C. O. Dietrich-Buchecker, J. Guilhem, C. Pascard, J.-P. Sauvage, *J. Chem. Soc., Chem. Commun.* **1985**, 244; M. Cesario, C. O. Dietrich-Buchecker, A. Edel, J. Guilhem, J.-P. Kintzinger, C. Pascard, J.-P. Sauvage, *J. Am. Chem. Soc.* **1986**, *108*, 6250; A. M. A. Gary, C. O. Dietrich-Buchecker, Z. Saad, J.-P. Sauvage, *J. Am. Chem. Soc.* **1988**, *110*, 1467; A. Livoreil, C. O. Dietrich-Buchecker, J.-P. Sauvage, *J. Am. Chem. Soc.* **1994**, *116*, 9399; D. J. Cárdenas, A. Livoreil, J.-P. Sauvage, *J. Am. Chem. Soc.* **1996**, *118*, 11980; F. Baumann, A. Livoreil, W. Kaim, J.-P. Sauvage, *Chem. Commun.* **1997**, *35*; A. Livoreil, J.-P. Sauvage, N. Amaroli, V. Balzani, L. Flamigni, B. Ventura, *J. Am. Chem. Soc.* **1997**, *119*, 12114; J.-C. Chambron, J.-P. Sauvage, K. Mislow, A. De Cian, J. Fischer, *Chem. – Eur. J.* **2001**, *7*, 4085.

[4] D. A. Leigh, P. J. Lusby, S. J. Teat, A. J.Wilson, J. K. Y. Wong, *Angew. Chem.* **2001**, *113*, 1586; *Angew. Chem., Int. Ed.* **2001**, *40*, 1538.

[5] B. L. Allwood, N. Spencer, H. Shahriari-Zavareh, J. F. Stoddart, D. J. Williams, *J. Chem. Soc., Chem. Commun.* **1987**, 1064; P. R. Ashton, I. Iriepa, M. V. Reddington, N. Spencer, A. M. Z. Slawin, J. F. Stoddart, D. J. Williams, *Tetrahedron Lett.* **1994**, *35*, 4835; M. Asakawa, P. R. Ashton, S. E. Boyd, C. L. Brown, S. Menzer, D. Pasini, J. F. Stoddart, M. S. Tolley, A. J. P. White, D. J. Williams, P. G. Wyatt, *Chem. – Eur. J.* **1997**, *3*, 463.

[6] A. G. Kolchinski, D. H. Busch, N. W. Alcock, *J. Chem. Soc., Chem. Commun.* **1995**, 1289; P. R. Ashton, P. J. Campell, E. J. T. Chrystal, P. T. Glink, S. Menzer, D. Philp, N. Spencer, J. F. Stoddart, P. A. Tasker, D. J. Williams, *Angew. Chem.* **1995**, *107*, 1997; *Angew. Chem., Int. Ed.* **1995**, *34*, 1865; P. R. Ashton, E. J. T. Chrystal, P. T. Glink, S. Menzer, C. Schiavo, J. F. Stoddart, P. A. Tasker, D. J. Williams, *Angew. Chem.* **1995**, *107*, 2001; *Angew. Chem., Int. Ed.* **1995**, *34*, 1869; P. T. Glink, C. Schiavo, J. F. Stoddart, D. J. Williams, *J. Chem. Soc., Chem. Commun.* **1996**, 1483; P. R. Ashton, A. N. Collins, M. C. T. Fyfe, S. Menzer, J. F. Stoddart, D. J. Williams, *Angew. Chem.* **1997**, *109*, 760; *Angew. Chem., Int. Ed.* **1997**, *36*, 735; F. G. Gatti, D. A. Leigh, S. A. Nepogodiev, A. M. Z. Slawin, S. J. Teat, J. K. Y. Wong, *J. Am. Chem. Soc.* **2001**, *123*, 5983; A. M. Brouwer, C. Frochot, F. G. Gatti, D. A. Leigh, L. Mottier, F. Paolucci, S. Roffia, G. W. H. Wurpel, *Science (Washington, D.C.)* **2001**, *291*, 2124.

[7] F. Vögtle, S. Meier, R. Hoss, *Angew. Chem*. **1992**, *104*, 1628; *Angew. Chem., Int. Ed.* **1992**, *31*, 1619; S. Ottens-Hildebrandt, S. Meier, W. Schmidt, F. Vögtle, *Angew. Chem*. **1994**, *106*, 1818; *Angew. Chem., Int. Ed.* **1994**, *33*, 1767; S. Ottens-Hildebrandt, M. Nieger, K. Rissanen, J. Rouvinen, S. Meier, G. Harder, F. Vögtle, *J. Chem. Soc., Chem. Commun*. **1995**, 777; H. Adams, F. J. Carver, C. A. Hunter, *J. Chem. Soc., Chem. Commun*. **1995**, 809; A. G. Johnston, D. A. Leigh, R. J. Pritchard, M. D. Deegan, *Angew. Chem.* **1995**, *107*, 1324; *Angew. Chem., Int. Ed.* **1995**, *34*, 1209; A. G. Johnston, D. A. Leigh, L. Nezhat, J. P. Smart, M. D. Deegan, *Angew. Chem.* **1995**, *107*, 1327; *Angew. Chem., Int. Ed.* **1995**, *34*, 1212; Y. Geerts, D. Muscat, K. Müllen, *Macromol. Chem. Phys.* **1995**, *196*, 3425; D. A. Leigh, K. Moody, J. P. Smart, K. J. Watson, A. M. Z. Slawin, *Angew. Chem*. **1996**, *108*, 326; *Angew. Chem., Int. Ed.* **1996**, *35*, 306; D. Muscat, A. Witte, W. Köhler, K. Müllen, Y. Geerts, *Macromol. Rapid Commun*. **1997**, *18*, 233; T. Dünnwald, A. H. Parham, F. Vögtle, *Synthesis* **1998**, *3*, 339; T. Schmidt, R. Schmieder, W. M. Müller, B. Kiupel, F. Vögtle, *Eur. J. Org. Chem*. **1998**, 2003; A. H. Parham, R. Schmieder, F. Vögtle, *Synlett* **1999**, *12*, 1887; O. Safarowsky, E. Vogel, F. Vögtle, *Eur. J. Org. Chem*. **2000**, 499.

[8] O. Safarowsky, M. Nieger, R. Fröhlich, F. Vögtle, *Angew. Chem*. **2000**, *112*, 1699; *Angew. Chem., Int. Ed.* **2000**, *39*, 1616; F. Vögtle, A. Hünten, E. Vogel, S. Buschbeck, O. Safarowsky, J. Recker, A.-H. Parham, M. Knott, W. M. Müller, U. Müller, Y. Okamoto, T. Kubota, W. Lindner, E. Francotte, S. Grimme, *Angew. Chem*. **2001**, *113*, 2534; *Angew. Chem., Int. Ed*. **2001**, *40*, 2468.

[9] G. M. Hübner, J. Gläser, C. Seel, F. Vögtle, *Angew. Chem.* **1999**, *111*, 395; *Angew. Chem., Int. Ed.* **1999**, *38*, 383; see also C. Reuter, W. Wienand, G. M. Hübner, C. Seel, F. Vögtle, *Chem. – Eur. J.* **1999**, *5*, 2692; C. Reuter, F. Vögtle, *Org. Lett*. **2000**, *2*, 593; G. M. Hübner, C. Reuter, C. Seel, F. Vögtle, *Synthesis* **2000**, *1*, 103; C. Seel, F. Vögtle, *Chem. – Eur. J.* **2000**, *6*, 21.

[10] C. Seel, A. H. Parham, O. Safarowsky, G. M. Hübner, F. Vögtle, *J. Org. Chem*. **1999**, *64*, 7236.

[11] A. Affeld, G. M. Hübner, C. Seel, C. A. Schalley, *Eur. J. Org. Chem*. **2001**, 2877; H. W. Gibson, S. Liu, P. Lecavalier, C. Wu, Y. X. Shen, *J. Am. Chem. Soc*. **1995**, *117*, 852; P. R. Ashton, R. Ballardini, V. Balzani, M. Bělohradský, M. T. Gandolfi, D. Philp, L. Prodi, F. M. Raymo, M. V. Reddingon, N. Spencer, J. F. Stoddart, M. Venturi, D. J. Williams, *J. Am. Chem. Soc*. **1996**, *118*, 4931; M. Asakawa, P. R. Ashton, R. Ballardini, V. Balzani, M. Bělohradský, M. T. Gandolfi, O. Kocian, L. Prodi, F. M. Raymo, J. F. Stoddart, M. Venturi, *J. Am. Chem. Soc*. **1997**, *119*, 302; P. R. Ashton, I. Baxter, M. C. T. Fyfe, F. M. Raymo, N. Spencer, J. F. Stoddart, A. J. P. White, D. J. Williams, *J. Am. Chem. Soc.* **1998**, *120*, 2297; C. Heim, Ph.D. Thesis, University of Bonn, 1998; C. Heim, A. Affeld, M. Nieger, F. Vögtle, *Helv. Chim. Acta* **1999**, *82*, 746; G. M. Hübner, G. Nachtsheim, Q.-Y. Li, C. Seel, F. Vögtle, *Angew. Chem*. **2000**, *112*, 1315; *Angew. Chem., Int. Ed*. **2000**, *39*, 1269.

[12] S. J. Weiner, P. A. Kollman, D. A. Case, U. C. Singh, G. Alagona, S. Profeta, P. Weiner, *J. Am. Chem. Soc*. **1984**, *106*, 765; S. J. Weiner, P. A. Kollman, N. T.Nguyen, D. A. Case, *J. Comput. Chem*. **1987**, *7*, 230; D. M. Ferguson, P. A. Kollman, *J. Comput. Chem*. **1991**, *12*, 620.

[13] Schrödinger, Inc., 1500 SW First Avenue, Suite 1180, Portland, OR 97201, USA; see also F. Mohamadi, N. G. Richards, W. C. Guida, R. Liskamp, C. Caulfield, G. Chang, T. Hendrickson, W. C. Still, *J. Comput. Chem*. **1990**, *11*, 440; D. Q. McDonald, W. C. Still, *Tetrahedron Lett*. **1992**, *33*, 7743.

[14] C. A. Hunter, *J. Chem. Soc., Chem. Commun*. **1991**, 749; C. A. Hunter, *J. Am. Chem. Soc*. **1992**, *114*, 5303; F. Vögtle, S. Meier, R. Hoss, *Angew. Chem*. **1992**, *104*, 1628; *Angew. Chem., Int. Ed.* **1992**, *31*, 1619.

[15] G. Baddeley, M. A. Vickars, *J. Chem. Soc*. **1963**, 765; A. R. van Doorn, M. Bos, S. Harkema, J. van Eerden, W. Verboom, D. N. Reinhoudt, *J. Org. Chem*. **1991**, *56*, 2371.

Received December 17, 2001